ABSTRACT

MEDENBLIK, ANDREA STEWART. Determination of Soil and Tree Water Sources and Residence Times Using Stable Isotopes in a Southern Appalachian Forest. (Under the direction of Dr. Ryan E. Emanuel).

Climate change and population growth are major challenges to drinking water availability and sustainable water management. Even small shifts in climate can cause substantial changes in extreme weather events, affecting quantities and patterns of available drinking water. Soil moisture is a critical component of the hydrologic cycle that controls surface water movement, aquifer recharge, and water quality. Water in the unsaturated zone plays a key role in ecosystem function by mediating plant water uptake, plant nutrient availability, nutrient leaching, and biogeochemical processes. Forest extent and composition are additional key factors to managing water supplies, as the majority of water supply in the United States originates on forested land. Rising temperatures may increase plant water use via transpiration and evaporation, leaving less water for streamflow and groundwater recharge.

Hydrologic models are useful tool to predict changes in hydrological processes and water supply due to climate and land use dynamics. Many watershed models simplify biological processes associated with plant water uptake and transpiration, often assuming that roots uptake water from the same moisture pool that feeds the stream. Several studies using the stable isotope of water have suggested that this assumption may be incorrect due to incomplete mixing of subsurface waters. However, tree water use has not been explored using stable isotopes in humid watersheds with low seasonable variability. Additionally, a key issue in studies of ecohydrologic separation has been the collection of mobile soil water. The extent to which the methods used to collect soil water affects the isotope composition of those samples is unknown. To fully

characterize plant water uptake and aid hydrologic models, we must use appropriate methods to collect soil water and understand the seasonal isotopic dynamics of soil water.

In this study, we use a factorial experiment to demonstrate how characteristics of falling-tensions lysimeters impact the volume and stable isotope composition of collected soil waters in a humid, southern Appalachian site. We show that initial applied tension, sample duration, and lysimeter length significantly influence lysimeter sample volume but not isotope composition. We also show that seasonal origin and age of extracted water was significantly influence by season and soil depth. We apply these findings to the lysimeter methods of an additional experiment nearby, which collected seasonal samples of soil water, precipitation, stream water, ground water, and tree water. We show that tree water sources and residence times significantly vary by tree species in a humid catchment. Our results suggest the existence of two distinct pools of water whose physical characteristics evolve through time and reflect new inputs of precipitation and mixing of existing soil water. Additionally, our findings have implications for drought vulnerability and forest management, as species that rely on young water for transpiration may be more susceptible to dry periods.

Determination of Soil and Tree Water Sources and Residence Times Using Stable Isotopes in a Southern Appalachian Forest

by
Andrea Stewart Medenblik

A thesis submitted to the Graduate Faculty of
North Carolina State University
in partial fulfillment of the
requirements for the degree of
Master of Science

Natural Resources

Raleigh, North Carolina
2019

APPROVED BY:

Dr. Ryan E. Emanuel Committee Chair	Dr. Elizabeth G. Nichols
Dr. James M. Vose	Dr. Andrew C. Oishi External Member

DEDICATION

This thesis is first dedicated to my parents, Randy and Anne Stewart, who have encouraged me in all my pursuits, educational and otherwise. They unintentionally fostered a natural love and appreciation for water and forests that has guided my career. I will forever be indebted to them. My sister, Lauren, has been a constant friend and fervent listener. I am especially grateful for my patient husband, Jonathan, who not only tolerated my time in graduate school but also provided unending support and inspiration. I dedicate this work to all the classmates, colleagues, friends, and family members who shared words of encouragement and acts of kindness during this journey.

I would also like to recognize those who guided my academic pathway. I thank Mrs. Sharyl Cole, Mr. William Oliver, and Mr. Mitch Cox, for shaping my writing skills. Mr. Jeff Faulkner and Mrs. Becky Smith demonstrated the excitement and power of science. Stephen Keith, Dr. Benjamin Mirus, and Dr. Diego Riveros-Iregui provided the foundation I needed to study ecohydrology. I am grateful to advisors Dr. Geoff Bell, Dr. Karen Kandl, Dr. Katherine Elliott, and Dr. Lawrence Band, who taught me what it means to do research. I dedicate my thesis to all these individuals who indirectly supported its production.

BIOGRAPHY

Andrea Stewart Medenblik grew up in Hillsborough, North Carolina and attended Orange High School. Following her interests in conservation and the environment, she attended the University of North Carolina at Chapel Hill to receive a Bachelor of Science in Environmental Science with minors in Computer Science and Geography in 2016. Throughout her undergraduate career, she interned and conducted research at the North Carolina Botanical Garden, the Virginia Tech StREAM Lab, Coweeta Hydrologic Laboratory, UNC Environment Health and Safety, and AECOM. Andrea began her master's program in Dr. Ryan Emanuel's Ecohydrology and Watershed Science lab in 2016 as a National Science Foundation Graduate Research Fellow. She is currently a student hydrologist at the U.S. Geological Survey South Atlantic Water Science Center.

ACKNOWLEDGMENTS

First and foremost, I would like to acknowledge and thank my advisor, Dr. Ryan Emanuel, for guiding my graduate career from its earliest stages, providing timely mentorship, challenging me to answer scientific questions from creative angles, encouraging high standards, and inspiring me with his passion for hydrology and environmental issues. I also gratefully acknowledge the other members of my committee, Dr. Elizabeth Nichols, Dr. Jim Vose, and Dr. Chris Oishi, for providing constructive feedback and encouragement.

This thesis would not have been possible without the support of Coweeta Hydrologic Laboratory. Comments and project development input from Dr. Jennifer Knoepp and Dr. Chelcy Miniat were central in shaping this work. Thank you to Jason Love, Chris Sobek, Katherine Bower, Danielle Thornton, and others for field and equipment assistance.

Special thanks to Theo Jass, who provided substantial assistance by analyzing samples in the lab, maintaining equipment, assisting with project development, and helping with field work.

Funding was provided by the National Science Foundation Long-Term Ecological Research program granted to the Coweeta LTER Program at the University of Georgia and the National Science Foundation Graduate Research Fellowship. Thank you also to the USDA Forest Service Southern Research Station for hosting this research and providing data.

TABLE OF CONTENTS

LIST OF TABLES

LIST OF FIGURES

CHAPTER 1: Introduction

For over a century, hydrologists have acknowledged that plants influence the patterns of water movement. Forests influence water yield and quality at the catchment scale, making them a key target for management of water resources. Though hundreds of catchment studies have acknowledged the importance of trees and forests in hydrologic processes (Bosch & Hewlett, 1982), little consideration has historically been given to the regulatory role that plants can play in water movement. Transpiration has been oversimplified and poorly parameterized in many hydrologic models, often aggregated to the catchment scale or larger. This thesis attempts to combine hydrology and forest tree biology to explicitly consider plants in catchment hydrology.

Forest transpiration is a function of not only plant physiology but also soil water content. Soil moisture mediates plant water uptake, provides nutrients, and is influenced by tree water use. Therefore, a discussion of tree water use also necessitates a discussion of soil water content at a similar scale. Using stable isotope tracers is a powerful method to combine these two domains. To characterize plant-water relations across the globe, much discussion has centered around the collection of soil water using multiple tools with a range of sampling frequencies in a variety of ecosystems (McDonnell, 2014). Questions remain on how soil water collection methods can be appropriately used in a stable isotope approach.

This thesis presents a case study to explain plant water use regimes by exploring soil water collection methods, soil water isotope dynamics, and tree water isotope dynamics. It adds to a growing body of literature but is unique in its setting, an ecologically diverse, temperature ecosystem with high year-round precipitation. This work includes spatially-intense sampling of sixty trees across for species, providing a more detailed perspective of plant water use than often

available in past studies. Additionally, I challenge existing methods in stable isotope hydrology that were developed for semi-arid, Mediterranean, or seasonally variable climates.

I present my findings in two chapters: Chapter 2 explores how the specific methods applied to falling-tension lysimetry influences the sample volume and isotope composition of extracted soil water samples. It also defines the seasonality of sample volume and soil water isotope composition across multiple soil layers. These results inform future studies that use falling-tension lysimeters, including the following chapter. Chapter 3 uses the stable isotopes of precipitation, soil water, stream water, groundwater, and tree xylem water to explain the behavior of plant water uptake in a southern Appalachian hillslope. Together these chapters inform the isotope dynamics of soil water and tree water, two of the most variable pools in the hydrologic cycle, which can aid modeling efforts and our general understanding of transpiration in humid, temperate forests.

REFERENCES

Bosch, J.M. & Hewlett, J.D. (1982). A review of catchment experiments to determine the effect of vegetation changes on water yield and evapotranspiration. *Journal of Hydrology 55*(1-4): 3-23. doi: 10.1016/0022-1694(82)90117-2.

McDonnell, J.J. (2014). The two water worlds hypothesis: ecohydrological separation of water between streams and trees? *WIREs Water 1*(4): 323-329. doi: 10.1002/wat2.1027.

CHAPTER 2: The Influence of Experimental Design and Seasonality on the Volume and Stable Isotope Composition of Mobile Soil Water Sampled by Falling Tension Lysimetry

Abstract

Soil moisture is a critical pool of the hydrologic cycle that controls surface water movement, aquifer recharge, and water quality. Soil water plays a key role in ecosystem function by mediating plant water uptake, plant nutrient availability, nutrient leaching, and biogeochemical processes. It can also be used to infer physical characteristics of soil water related to source and age. Numerous collection techniques have been employed to examine these important soil water functions. Falling-tension lysimeters have been commonly used to collect soil water since the 1960s due to their low cost and ease of use. However, few studies have examined the influence of specific falling-tension lysimeter methods on the characteristics of extracted water. Here we show that initial applied tension, sample duration, and lysimeter length significantly influence lysimeter sample volume. We observed seasonal differences in sample volume and differences in the stable isotope composition ($\delta^{18}O$ and $\delta^{2}H$) of water extracted from two different soil depths across different seasons. The seasonal origin and age of extracted water was influenced significantly by season and soil depth. Though most lysimeter method manuals do not specify exact characteristics, our results indicate that lysimeter characteristics should be carefully chosen to accommodate desired collection volumes. Our findings suggest that our multiple lysimeter cup depths sample distinct pools of water whose physical characteristics evolve through time and reflect new inputs of precipitation and mixing of existing soil water. Beyond experimental design choice, our results reveal seasonal soil water dynamics and have implications for plant water availability.

Introduction

The quantity and quality of water in the unsaturated zone is crucial for human drinking water supply and ecosystem function. Despite comprising only approximately 0.05% of global freshwater resources (Shiklomanov, 1993), soil moisture is a critical pool that controls surface water movement, aquifer recharge, and water quality (Fetter, 2001). At the watershed scale, soil water storage induces strong memory effects, where past precipitation may influence rainfall-runoff relationships years into the future (Nippgen et al., 2016). Further, soil water can indicate plant water uptake (Cowan, 1965; Gardner, 1960; Miller, 1967; Ritchie, 1981), plant nutrient availability (Barber, 1995; Kramer, 1969; Tracy & Marin, 1989), nutrient leaching (Casey et al., 2002; Kolenbrander, 1969; Stagnitti et al., 2003), and biogeochemical processes (Austin et al., 2004; Chorover et al., 2007; Skopp et al., 1990). Additionally, we can use soil water to infer physical characteristics of soil water related to source and age through stable isotope analysis (e.g. Botter et al., 2011; Hrachowitz et al., 2013; Kirchner, 2016; McDonnell et al., 2010; Sprenger et al., 2018).

Clearly, soil water plays a key role in the study of ecosystem function. Numerous soil water collection techniques have been employed for over a century. In situ sampling methods include falling-tension lysimeters, zero-tension lysimeters, passive capillary wick samplers, pan lysimeters, suction plates, resin boxes, and others (Weihermüller, 2007). Falling-tension lysimeters, also called suction lysimeters, vacuum lysimeters, ceramic porous cup lysimeters, or rhizons, have been commonly used to collect soil water since the 1960s (Litaor, 1988). They consist of a porous ceramic cup attached at one end of a pipe; a partial vacuum is applied to extract freely draining water and slightly bound pore water (Briggs and McCall, 1904). Although previous studies have extensively compared soil water sampling methods and their relative

effects on sample volume, nutrient content, and isotope composition (Fares et al., 2009; Litaor, 1988; Sprenger et al., 2015; Weihermüller, 2007), few studies have examined the influence of specific parameters within falling-tension lysimeter methods.

The characteristics of falling-tension lysimeters, including the applied tension, sample duration, and lysimeter geometry, have been discussed in several studies. Severson and Grigal (1976) argue that applied tension should be the lowest possible value that allows sample collection, whereas others suggest that any tension between 0.03 and 0.08 MPa is sufficient (Paramasivam, 1997). In general, the tension to be applied to the porous cup depends on the soil type, amount of water desired for analysis, soil water content, and sample duration (Warrick & Ammozegar-Fard, 1977; Weihermüller, 2005). Sample durations in past experiments vary from several hours (Corwin, 2002) to months (Allen et al., 2019). Installation depth another lysimeter characteristic for consideration—studies typically recommend at least two lysimeter depths, one within the root zone and one below the root zone. Despite the extensive description of lysimeter methods in the literature, the influence of individual and combined lysimeter characteristics on sample volume and isotope composition has not been explored.

The isotopes of hydrogen and oxygen in water vary based on time, water source, and the movement of water, so examining the ratio of heavy to light isotopes can help discern the origin and age of soil water (Barnes & Turner, 1998). These natural tracers in soil water have been used to describe a range of processes, including groundwater recharge, root water uptake, preferential flow, and evaporation, that occur in the critical zone between groundwater and atmosphere (Sprenger, 2016). Several techniques have emerged to quantify these hydrologic fluxes and intra-annual isotopic variability. The Seasonal Origin Index (SOI) describes the season in which lysimeter soil water originated as precipitation (Allen et al., 2019). Similarly, the young water

fraction estimates the proportion of soil water that recently entered the unsaturated zone (Kirchner, 2016). These methods avoid common pitfalls related to spatial heterogeneity that affect older techniques such as travel time distribution and mean transit time (Kirchner, 2016). By applying the stable isotopes of hydrogen and oxygen to the SOI and young water fraction, we can better understand the composition of soil water and its seasonal behavior.

We sampled soil water monthly for one year to determine the effects of lysimeter characteristics on sample volume and stable isotope composition of oxygen and hydrogen. We assessed results from an array of falling-tension lysimeters representing a full factorial of three lysimeter lengths, three tensions, three sample durations, and two depths, collecting 1944 soil water samples total. Further, we compared soil water isotope data to precipitation isotope data to evaluate seasonal origin and fraction of young water. This study addresses the following questions: (a) How do lysimeter characteristics impact the volume of soil water samples? (b) How do lysimeter characteristics impact the isotope composition of soil water samples? (c) What is the annual variability of soil water isotope composition?

Methods

1. Site Description

This study was conducted at Coweeta Hydrologic Laboratory, a U.S. Forest Service Experimental Forest located in the Nantahala Mountain Range of western North Carolina and Blue Ridge physiographic province of the southern Appalachians (latitude 35°03' N, longitude 83°25' W) (Swank & Crossley, 1988). Climate in the Coweeta basin is classified as marine humid temperature due to high moisture and mild temperatures (Swift et al., 1988). The mean annual temperature is 12.6 °C, with mean monthly temperatures ranging from 2.9 °C to 21.8 °C

(Miniat et al., 2015). The average growing season extends from early May to early October (Swift et al., 1988). Annual precipitation is abundant, averaging approximately 1,800 mm and comprising less than 10% snowfall. Precipitation is greatest during the dormant season (Miniat et al., 2017).

Soils in the Coweeta basin are generally deep sandy loams underlain by folded schist and gneiss. Soils in the basin are either immature Inceptisols, found on steep slopes at high elevation, or older developed Ultisols, found on both steep ridges and gentle slopes (Swank & Crossley, 1988). The Saunook soil series, defined by fine-loamy, mixed, superactive, mesic Humic Hapludults, was the most prevalent soil type in the study site at the base of the Coweeta basin (Soil Survey Staff, 2018). These well-drained soils have moderately high to high saturated hydraulic conductivity, moderate permeability, and negligible surface runoff (National Cooperative Soil Survey, 2004). Depth to bedrock is approximately 6 m (Swank and Douglass, 1975), and depth to refusal ranges from 0.9 to 3.5 m below the surface (Singh et al., 2016). Although Coweeta exhibits a large elevation range (U.S. Geological Survey, 2009), the study site, a level riparian valley bottom at approximately 690 m elevation, was chosen to minimize the influence of elevation and associated topographic wetness (Figure 2.1).

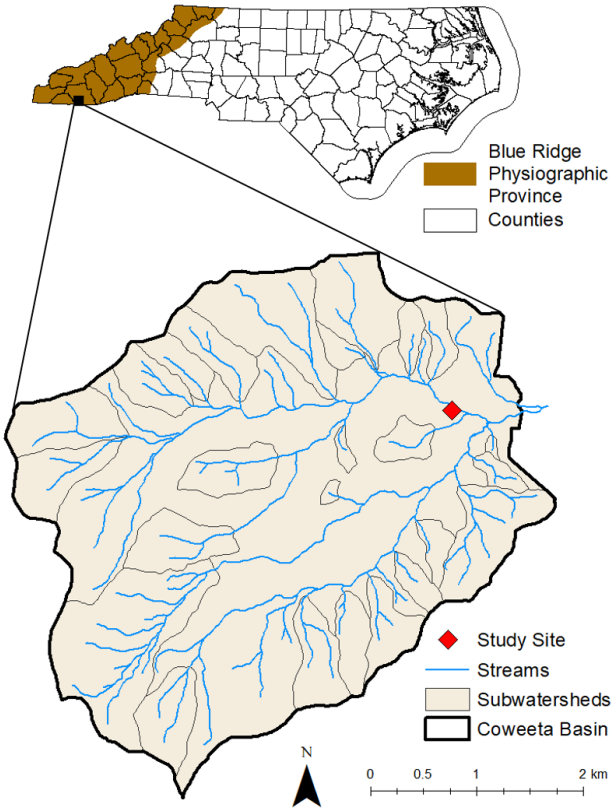

Figure 2.1. Site map at Coweeta Hydrologic Laboratory, North Carolina in the Blue Ridge physiographic province of the southern Appalachian Mountains.

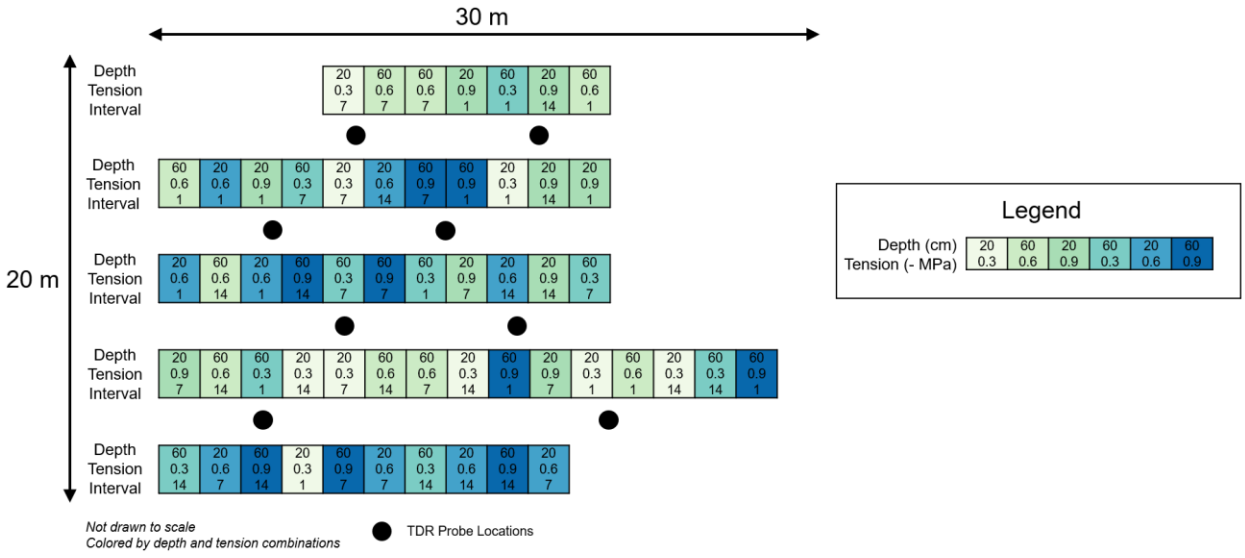

Figure 2.2. Schematic diagram of experimental design. Lysimeter depth (cm), tension (MPa), and sampling interval (d) were randomly assigned to one square meter plots along five transects. Plot color corresponds to depth-tension combinations. Two pairs of time-domain reflectometer (TDR) probes at 0-30 cm and 30-60 cm depths were installed between each transect.

2. Experimental Design

We used an array of 54 falling-tension lysimeters installed by the US Forest Service staff to represent a full factorial of several lysimeter characteristics. Lysimeters were PVC tubes with outside diameter of 4.8 cm capped with two-hole rubber stoppers and epoxied to porous clay cups (Soilmoisture Equipment Corp., Santa Barbara, USA). Teflon tubing in the stopper and Nalgene plastic tubing inside the PVC tubing permitted vacuum application and sample extraction. Three PVC tube lengths were used for lysimeter bodies: 40, 70, and 100 cm. Lysimeters were installed with their cups at one of two depths: 20 cm (within the root zone) or 60 cm (below the root zone). One of three initial tensions was applied to each lysimeter: -0.03, -0.06, or -0.09 MPa. Water was extracted after one of three sample intervals: 1, 7, or 14 days. Each unique lysimeter was sampled three times per month in 2013, comprising 162 soil water samples per month and 1944 soil water samples total.

Lysimeter depth, tension, and sampling interval were randomly assigned to one square meter plots along five transects within the study site (Figure 2.2). Lysimeters of all three lengths were placed in each plot. Lysimeters were installed by hand-augering holes to the desired depth, retaining the soil removed by depth, mixing the deepest soil with silica flour and deionized water to form a thick slurry, pouring the slurry in the hole, installing the lysimeter, and backfilling the hole with the remaining removed soil. Lysimeters were allowed to equilibrate with surrounding soil before beginning the year-long experiment. Tensions of -0.03 and -0.06 MPa were applied with a hand pump, and tensions of -0.09 MPa required an electric pump. Following the defined sample duration, water samples were extracted by hand pump and split into multiple containers for various analyses, including 20 mL glass vials sealed with a cone top cap to eliminate

headspace and avoid isotopic fractionation. When less than 20 mL of water was available for isotope analysis, samples were excluded from this study.

We monitored volumetric soil water content at the site using pairs of time-domain reflectometer (TDR) probes (Model CS-650, Campbell Scientific, Logan, UT) installed at 0-30 cm and 30-60 cm depths. Two pairs were placed between each transect for a total of 8 probe pairs (Figure 2.2). Observations from the probes were recorded at 15-minute intervals using a datalogger (Model CR1000, Campbell Scientific, Logan, UT). We obtained daily precipitation from a long-term climate station located approximately 200 m from the study site at a similar elevation.

We collected precipitation samples in bulk collectors distributed throughout the Coweeta basin. Collectors were constructed from 10 cm diameter polycarbonate rain gauges with a thin (5-10 mm) layer of mineral oil inside to prevent evaporation (Michelsen et al., 2018). Water samples were collected using a clean, dry polyethylene syringe and tubing to extract water from beneath mineral oil. We transferred water from the syringe into a 20 mL high-density polyethylene (HDPE) vials sealed with a cone top cap with no headspace. After sampling, precipitation collectors were cleaned and dried, and new mineral oil was added. Precipitation samples were collected every 1-4 weeks, depending on the total amount of precipitation. Total liquid water depth in the collector at the time of sampling was used to compute volume-weighted averages of precipitation $\delta^{18}O$ and $\delta^{2}H$ for each week. All precipitation isotopes are reported in volume-weighted values. Frozen precipitation occurred infrequently and was not included in this study.

3. Isotope Analysis

All soil water and precipitation samples were stored in a cool laboratory until analyzed in the lab. At the time of analysis, samples were transferred to 2 mL glass vials and analyzed for oxygen and hydrogen isotopes using a cavity ring-down laser spectrometer (model L2120-*i*, Picarro Inc., Santa Clara, CA, USA, ±0.05 ‰) equipped with an HTC PAL autosampler (LEAP Technologies, Inc., Carrboro, NC, USA). Isotope compositions ($\delta^{18}O$ and $\delta^{2}H$) were reported in per mil (‰) relative to a standard as

$$\delta^{18}\text{O or } \delta^{2}\text{H} = \left(\frac{R_{sample}}{R_{standard}} - 1\right) * 1000 \quad (1)$$

where *R* is the ratio of ^{2}H to ^{1}H atoms or ^{18}O to ^{16}O atoms of the sample and the lab standard. Internal lab standards were calibrated against International Atomic Energy Agency (IAEA) standards Vienna Standard Mean Ocean Water (VSMOW2, 0 ‰ $\delta^{18}O$ and 0 ‰ $\delta^{2}H$), Greenland Ice Sheet Precipitation (GISP, -24.76 ‰ $\delta^{18}O$ and -189.5 ‰ $\delta^{2}H$), and Standard Light Antarctic Precipitation (SLAP2, -55.50 ‰ $\delta^{18}O$ and -427.5 ‰ $\delta^{2}H$). Raw instrument data were corrected in MATLAB (R2018a, Mathworks, Inc., Natick, MA, USA) according to guidelines published by the IAEA Isotope Hydrology Laboratory (Tanweer et al., 2009). Instrument $\delta^{2}H$ accuracy was 0.95 ‰ and precision was 0.21 ‰, giving a total instrument $\delta^{2}H$ uncertainty of 1.17 ‰. Instrument $\delta^{18}O$ accuracy was 0.05 ‰ and precision was 0.05 ‰, resulting in total instrument $\delta^{18}O$ uncertainty of 0.10 ‰.

We used weekly depth- weighted precipitation $\delta^{18}O$ and $\delta^{2}H$ to generate a local meteoric water line (LMWL) for the year 2013, which took the form of $\delta^{2}H = 8.03 \times \delta^{18}O + 15.16$ (R^2 = 0.90) (Figure 2.8). The slope of the LMWL was similar to that of the global meteoric water line ($\delta^{2}H = 8 \times \delta^{18}O + 10$). The higher intercept of the LMWL suggests that moisture sources of precipitation events were altered during their transport from their origins (Clark & Fritz, 1997).

We used the SOI, developed by Allen et al. (2019), to characterize when lysimeter soil water originated as precipitation. SOI is defined as

$$\mathrm{SOI} = \begin{cases} \dfrac{\delta_x - \delta_{annP}}{\delta_{summerP} - \delta_{annP}}, \text{if } \delta_x > \delta_{annP} \\ \dfrac{\delta_x - \delta_{annP}}{\delta_{annP} - \delta_{winterP}}, \text{if } \delta_x < \delta_{annP} \end{cases} \quad (2)$$

where δ_x is the fractionation-compensated δ^2H isotopic signature of lysimeter soil water samples, and $\delta_{winterP}$, $\delta_{summerP}$, and δ_{annP} are the δ^2H isotopic signatures of typical winter, typical summer, and volume-weighted annual precipitation. We used iteratively reweighted least squares multiple regression on lysimeter sample δ^2H to calculate a measure of central tendency (*offset*) and strength of seasonal cycle (*amplitude*). Typical winter precipitation was defined as $\delta_{winterP}$ = *offset – amplitude,* and typical summer precipitation was defined as $\delta_{summerP}$ = *offset* + *amplitude*. To compensate for fractionation effects of δ_x, soil isotope values were adjusted back to the LMWL along an evaporation line slope, calculated by the Craig-Gordon model for diffusion-controlled soil evaporation scenarios by Bennetin et al. (2018). The SOI is near -1.0 for water samples derived entirely from winter precipitation, near 1.0 for sample derived entirely from summer precipitation, and near 0 if they represent a mixture of waters from all seasons. The SOI may exceed the bounds of -1 to 1 if intra-season variability is greater than inter-seasonal variability; a winter sample, for example, may be isotopically lighter than typical winter precipitation and have an SOI less than -1. This method differs from a simple, two-end member mixing model because it accounts for seasonal differences in precipitation amount; for example, we may expect to see more winter water than summer water in soil water samples if more precipitation falls during winter.

To further describe water age, we used the fraction of young water, described by Kirchner (2016), to quantify the percentage of soil water that entered the unsaturated zone as

precipitation in the last 2.3 ± 0.8 months. The basis of the young water fraction methods is the seasonal cycles of $\delta^{18}O$ in precipitation and soil water. We used cosine and sine waves to fit our precipitation and soil water data to seasonal cycle curves. Cosine and sine coefficients were calculated for soil water and precipitation by iteratively reweighted least squares multiple regression on $\delta^{18}O$ values for weekly depth-weighted precipitation and groups of lysimeter samples. The amplitude of each cycle was calculated by taking the square root of the sum of the squares of the cycle coefficients. The percentage of young water for each group of lysimeter samples was calculated by dividing the lysimeter $\delta^{18}O$ cycle amplitude by the precipitation $\delta^{18}O$ cycle amplitude and multiplying by 100. Young water percentages may be over 100% if the precipitation isotope record does not fully capture its variability due to low sample number. Young water percentage was capped at 100% in this study, which occurred in 14 groupings of soil water samples.

4. Statistical analysis

All data processing and statistical analyses were performed in R (R Core Team, 2018). Seventy-four soil water samples were excluded from isotope analysis because they were deemed outliers by Chauvenet's criterion or lab notes indicated that the sample had evaporated due to vial headspace or broken vials. We used the "kruskal.test" function to use the Kruskal-Wallis Test to compare medians and distributions of sample volume, isotope composition, SOI, and young water fraction. We used the "posthoc.kruskal.nemenyi.test" function as a post-hoc test to calculate pairwise multiple comparisons between group levels. We used the "lm" function to perform linear regression. We used a script provided by James Kirchner to perform iteratively

reweighted least squares multiple regression, which fit the isotope data to sine and cosine functions for SOI and water age analysis (Kirchner, 2016).

Results

1. Hydrologic Conditions

In 2013, mean daily temperature was 12.21 °C, ranging from 3.6 °C in February to 20.8 °C in July (Figure 2.3a). Mean monthly temperatures were typical of long-term records apart from January at 5.9 °C, 103% warmer than average, and March at 5.2 °C, 40% colder than average.

Precipitation was high relative to long-term records at Coweeta Hydrologic Laboratory. The total annual precipitation in 2013 was 2,384 mm, the second-wettest year on record and approximately 32% greater than the long-term average (1936 to 2018). Monthly precipitation was typical of long-term records apart from January at 428 mm, 151% higher than average for the month, and July at 428 mm, 204% higher than average for the month. Precipitation in January reached the all-time record for the month and can be attributed to one large storm on January 30 (Figure 2.3b). The late summer and early fall were dry, with only 224 mm of precipitation between August and October. Thus, the "second wettest year" designation can be attributed largely to storms in January and July.

2. Soil Physical Characteristics

Soil water retention characteristics were typical of sandy loam soils. Bulk density ranged from 1.2 to 1.4 g cm^{-3}, increasing with depth (Table 2.1). Soil water retention curves indicate that

the deeper soil has a greater distribution of pore sizes and exhibits characteristics more similar to sand, whereas the shallow soil is more similar to silty loam (Figure 2.4).

Table 2.1. Soil water retention characteristics at two depths.

Soil depth (cm)	Bulk density (g cm^{-3})	$H_2O_{saturation}$ (g cm^{-3})	$H_2O_{permanent\ wilting\ point}$ (g cm^{-3})
20	1.2	0.49	0.31
60	1.4	0.43	0.28

Soil water content responded to storms throughout the year (Figure 2.3c). Soil water content was lowest in fall and highest in summer winter. Mean daily soil water content in the shallow layer (0 – 30 cm depth) was 0.28 cm^3 cm^{-3}, ranging from 0.18 to 0.37 cm^3 cm^{-3}. Shallow soil water content was more responsive to storm events, especially during the dry fall season. Mean daily soil water content in the deep layer (30 – 60 cm depth) was 0.27 cm^3 cm^{-3}, ranging from 0.19 to 0.38 cm^3 cm^{-3}.

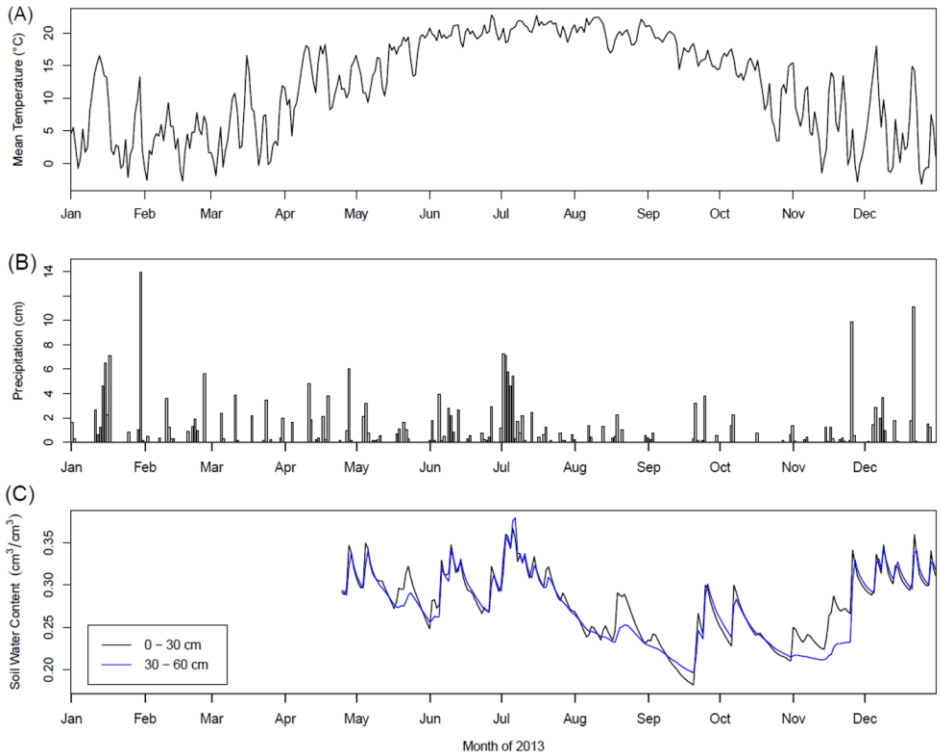

Figure 2.3. Hydroclimate data at Coweeta Hydrologic Laboratory in 2013. (A) Mean daily temperature (° C) at Climate Station 01 (CS01, latitude 35.07382, longitude -83.47845) (Miniat et al., 2015). (B) Mean daily precipitation (cm) at CS01. (C) Mean daily volumetric soil water content (cm^3 cm^{-3}), averaged over two depth ranges (0 – 30 cm and 30 – 60 cm).

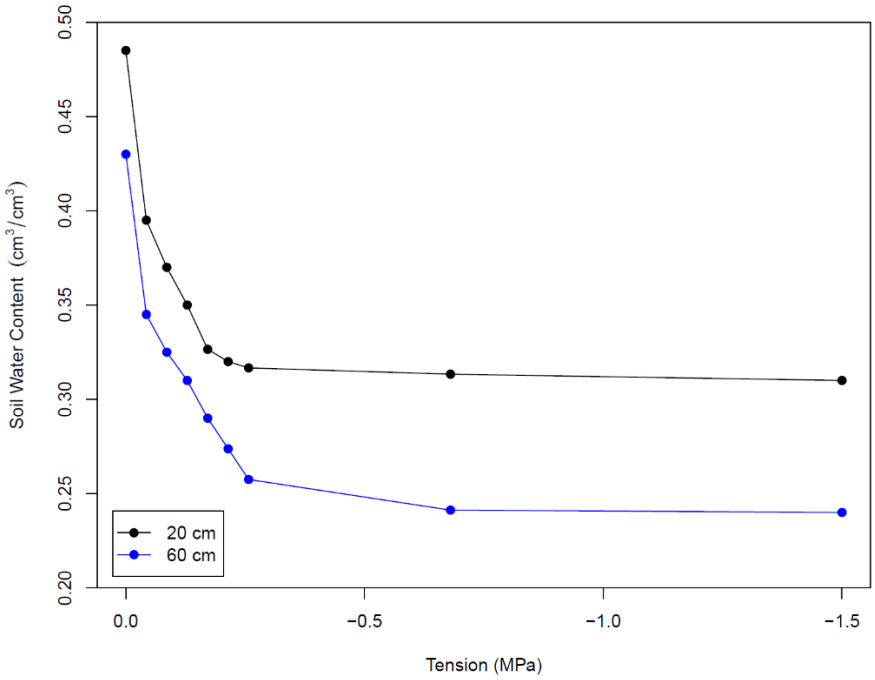

Figure 2.4. Soil water retention curve for soil at experimental site at two depths.

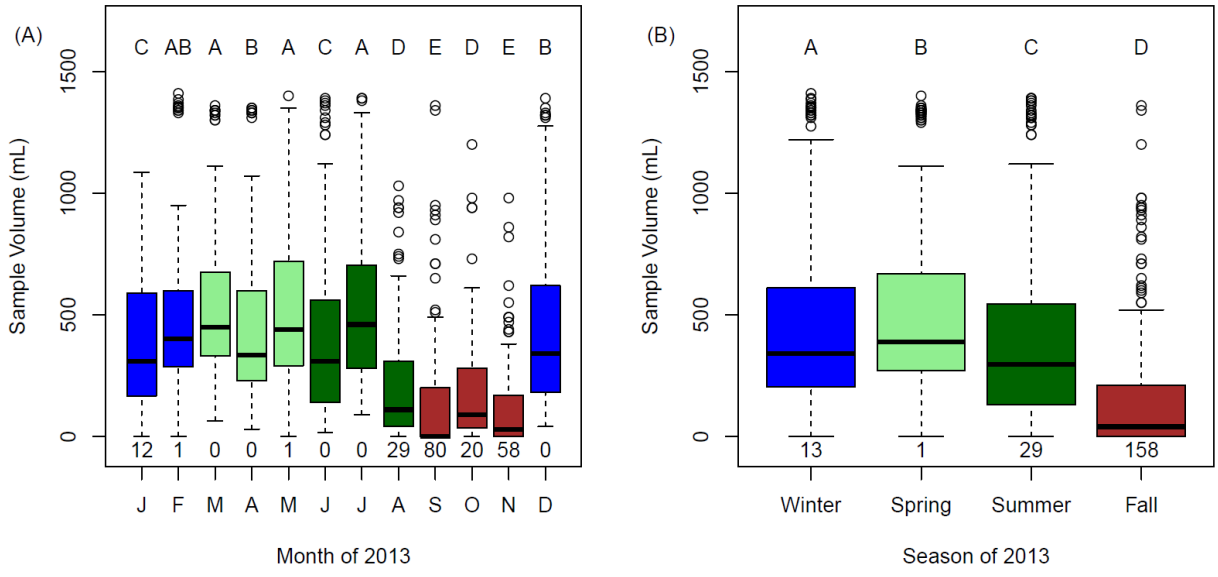

Figure 2.5. Distribution of sample volume by (A) month and (B) season of soil water sample. Samples are marked as outliers (shown as circles) if their value is outside 1.5 times the interquartile range above the upper quartile or below the lower quartile. The number of samples with zero volume is listed below each boxplot.

3. Influences of Lysimeter Characteristics and Seasonality on Sample Volume

The mean volume of all lysimeters samples collected was 382 mL per sample. Collection volume ranged from 0 mL to 1410 mL per sample. There were 202 dry samples (0 mL collected). August through November had significantly lower sample volume than the rest of the year with a mean sample volume of 167 mL (Figure 2.5a). Each season had a significantly different distribution of sample volumes ($p < 0.001$) (Figure 2.5b), with larger sample volumes collected in spring and smaller sample volumes collected in fall.

The influence of individual lysimeter characteristics on sample volume is displayed in Figure 2.6. Sample volume increased with initial tension, and differences in sample volumes were significant among tensions ($p < 0.001$). Similarly, sample volume increased with sample duration, and differences in sample volumes were significant among sample duration ($p < 0.001$). Sample volume also increased with lysimeter length. Lysimeters with 40 cm tubes collected less water than those with 70 cm or 100 cm tubes ($p < 0.001$), but 70 cm and 100 cm tube lengths did not yield significantly different sample volumes. Lysimeter cup installation depth alone did not significantly influence sample volume ($p = 0.16$); when not accounting for other factors, shallow and deep soils produced indistinguishable sample volumes.

The influence of combined lysimeter characteristics on sample volume is shown in Figure 2.7. The largest sample volumes were collected from lysimeters with a combination of 60 cm cup installation depth, 100 cm length, 14-day sample duration, and -0.09 MPa tension. The smallest sample volumes were collected from lysimeters with a combination of 20 cm cup installation depth, 40 cm length, 1-day sample duration, and -0.03 MPa tension. The largest sample volumes were collected in spring, followed by winter, summer, and fall.

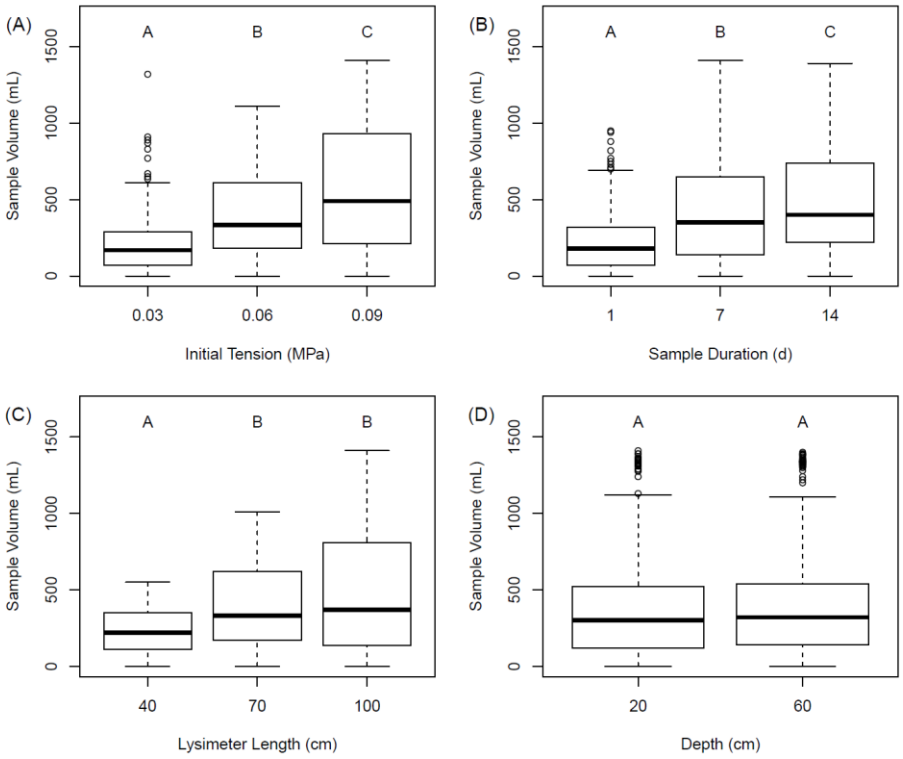

Figure 2.6. Distribution of sample volume by (A) initial lysimeter tension (MPa), (B) sample duration (d), (C) lysimeter length (cm), and (D) lysimeter depth (cm). Samples are marked as outliers (shown as circles) if their value is outside 1.5 times the interquartile range above the upper quartile or below the lower quartile.

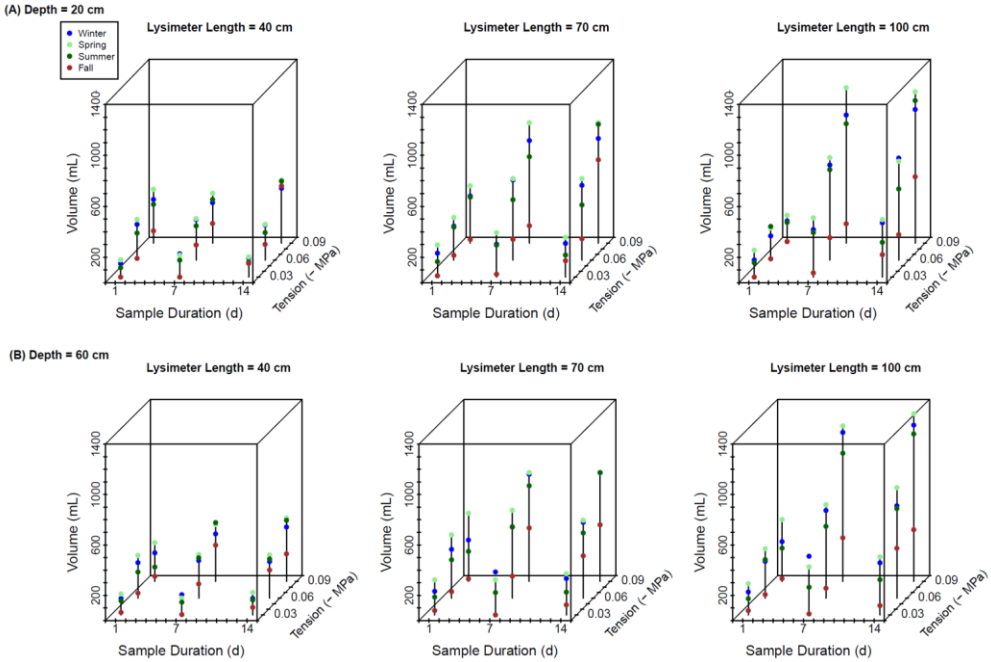

Figure 2.7. Average seasonal sample volume, separated by each combination of lysimeter depth (cm), lysimeter length (cm), sample duration (d), and initial lysimeter tension (MPa).

Multiple linear regression was used to investigate the interacting effects of lysimeter depth, lysimeter length, sample duration, initial vacuum, and season of sample. A model containing lysimeter length, sample duration, initial vacuum, and season produced the lowest Akaike's Information Criterion (AIC) value (Akaike, 1974). Table 2.2 reports model coefficients and significance values. The R^2 value was 0.351, and the adjusted R^2 value was 0.350. Residual standard error was 271 on 1760 degrees of freedom (Appendix A).

Table 2.2. Multiple linear regression model outputs for best fit model for sample volume.

Model Term	Value	SE	t-value	p-value
(Intercept)	80.30	26.18	3.07	N/A
Lysimeter Length (cm)	4.17	0.28	14.75	< 0.001
Sample Duration (d)	20.92	1.29	16.17	< 0.001
Season (Spring)	62.24	17.63	3.64	< 0.001
Season (Summer)	-51.22	17.85	-2.87	< 0.01
Season (Fall)	-294.58	18.74	-15.71	< 0.001

4. Influence of Lysimeter Characteristics on the Isotopic Composition of Soil Water

We used 82 precipitation samples collected in 2013 to generate a local meteoric water line (LMWL) that took the form of $\delta^2H = 8.03 \pm 0.50 \times \delta^{18}O + 15.16 \pm 3.06$ ($R^2 = 0.90$). The mean weekly isotope composition was -5.81 $\delta^{18}O$ ‰ and -31.53 δ^2H ‰. Precipitation isotope composition ranged from -2.59 $\delta^{18}O$ ‰ and -6.75 δ^2H ‰ in summer to -9.09 $\delta^{18}O$ ‰ and -57.48 δ^2H ‰ in winter.

A total of 1611 of 1944 lysimeter samples (83%) had sufficient volume to be analyzed for isotope composition. Most empty samples occurred in the dry fall season. Seventy-eight additional samples were excluded from analysis due to broken vials or large bubbles (> 1 mm diameter) assumed to cause evaporative enrichment. The mean soil water isotope composition was -5.81 $\delta^{18}O$ ‰ and -31.53 δ^2H ‰. The soil water regression line was $\delta^2H = 7.41 \pm 0.04 \times \delta^{18}O + 10.67 \pm 0.22$ ($R^2 = 0.96$), indicating that soil waters generally fell along the LMWL (Figure 2.8).

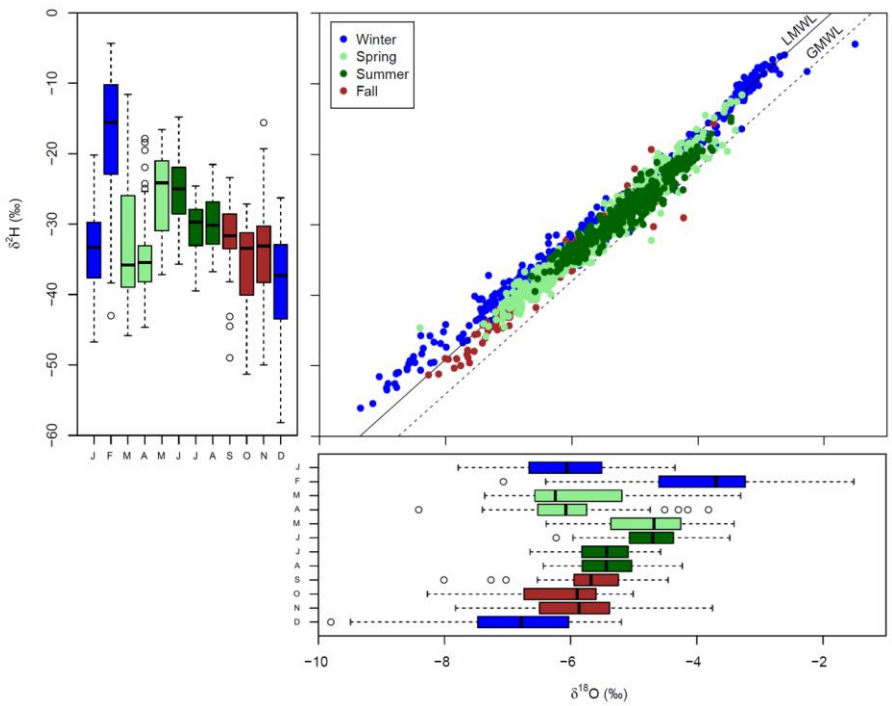

Figure 2.8. Dual isotope plot for all lysimeter samples, separated by season, and box plots for $\delta^{18}O$ and $\delta^{2}H$, separated by month. The local meteoric water line (LMWL, $\delta^{2}H = 8.03 \times \delta^{18}O + 15.16$) is shown with a solid line, and global meteoric water line (GMWL, $\delta^{2}H = 8 \times \delta^{18}O + 10$) is shown with a dashed line.

The isotope composition of all lysimeter water samples is shown in a dual isotope plot in Figure 2.8. Monthly and seasonal variability of $\delta^{2}H$ and $\delta^{18}O$ are also shown as box plots in Figure 2.8. On average, summer samples had the heaviest isotope composition and least variability, whereas winter samples were isotopically lighter and more variable. Each season had a significantly different distribution of $\delta^{18}O$ ($p < 0.001$) and $\delta^{2}H$ values ($p < 0.001$). Pairwise Kruskal-Wallis tests reveal that, with the exception of winter and spring, seasonal $\delta^{18}O$ and $\delta^{2}H$ values were significantly different.

The influence of individual lysimeter characteristics on sample isotope composition is displayed in Figure 2.9. The distribution of $\delta^{18}O$ values differed significantly among the two installation depths ($p < 0.001$). Samples collected from 60 cm depth were isotopically lighter and had less variability than samples from 20 cm depth. The distribution of $\delta^{18}O$ was not influenced

by initial tension (p = 0.32), sample duration (p = 0.52), or lysimeter length (p = 0.88). Isotope composition appeared to become less variable as sample duration increased, but the relationship was not significant.

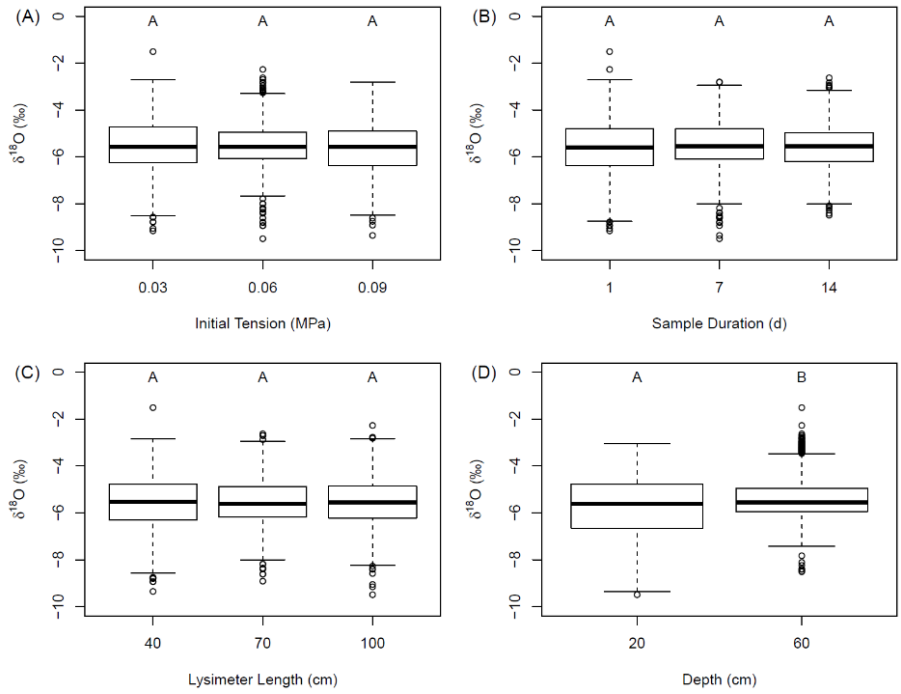

Figure 2.9. Distribution of sample $\delta^{18}O$ values by (A) initial lysimeter tension (MPa), (B) sample duration (d), (C) lysimeter length (cm), and (D) lysimeter depth (cm). Samples are marked as outliers (shown as circles) if their value is outside 1.5 times the interquartile range above the upper quartile or below the lower quartile.

5. Seasonal Origins of Soil Water

The mean SOI of lysimeter samples was 0.22, ranging from -11.19 to 3.71. Approximately one-third (28%) of samples had an SOI between -0.5 and 0.5, indicating that the isotopic composition was near the annual average precipitation and potentially represented many possible mixtures of water from all seasons. One third (34%) of samples had low (< -0.5) SOI values, indicating that at least half of the soil water originated from winter precipitation. Another third (38%) of samples had high (> 0.5) SOI values, meaning at least half of the soil water originated from summer precipitation.

Figure 2.10 shows the monthly and seasonal distribution of SOI. With the exception of February, summer months exhibited higher SOI values, and winter months exhibited lower SOI values. Each season had a significantly different distribution of SOI values ($p < 0.001$). In pairwise comparisons, each season was significantly different from each other except that winter was not significantly different from spring.

The influence of individual lysimeter characteristics on SOI is displayed in Figure 2.11. The lysimeter installation depths had significantly different SOI values ($p < 0.001$). Samples at 60 cm depth had less variability in seasonal origin than samples at 20 cm depth, with half of all values between -0.45 and 0.76. Samples at 20 cm depth were skewed towards lower SOI values. The distribution of SOI values was not influenced by initial tension ($p = 0.64$), sample duration ($p = 0.84$), or lysimeter length ($p = 0.64$). In all groupings, the median SOI was greater than 0 and the distribution of values favored summer precipitation origins.

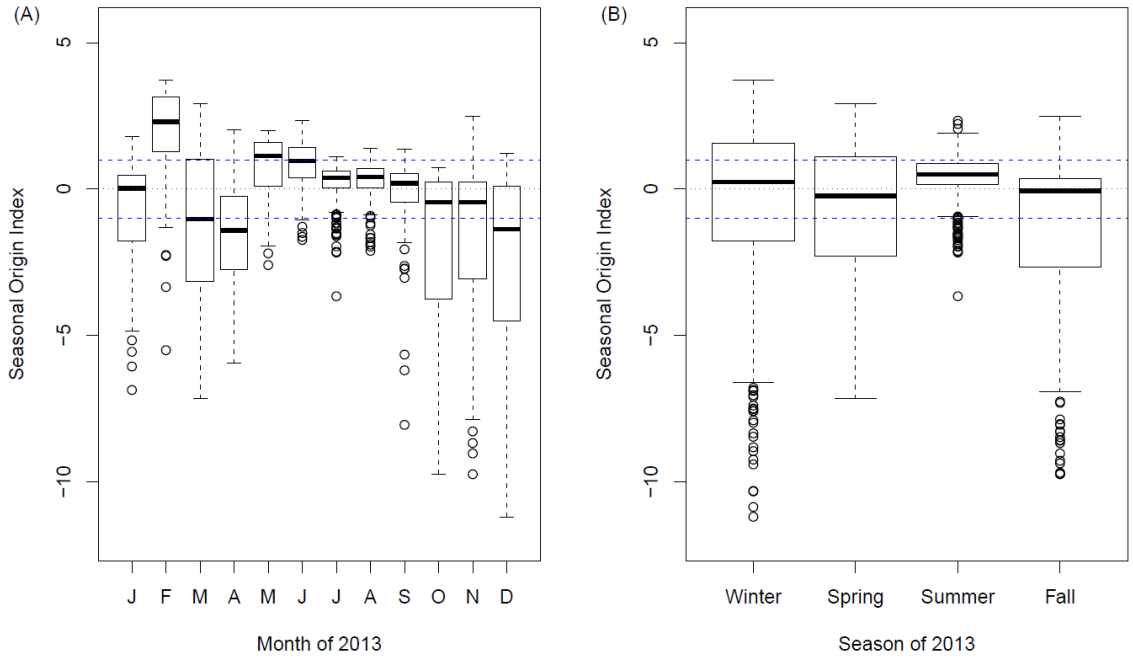

Figure 2.10. Distribution of Seasonal Origin Index by (A) month and (B) season of soil water sample. Samples are marked as outliers (shown as circles) if their value is outside 1.5 times the interquartile range above the upper quartile or below the lower quartile. SOI = ± 1 is marked by blue dashed lines.

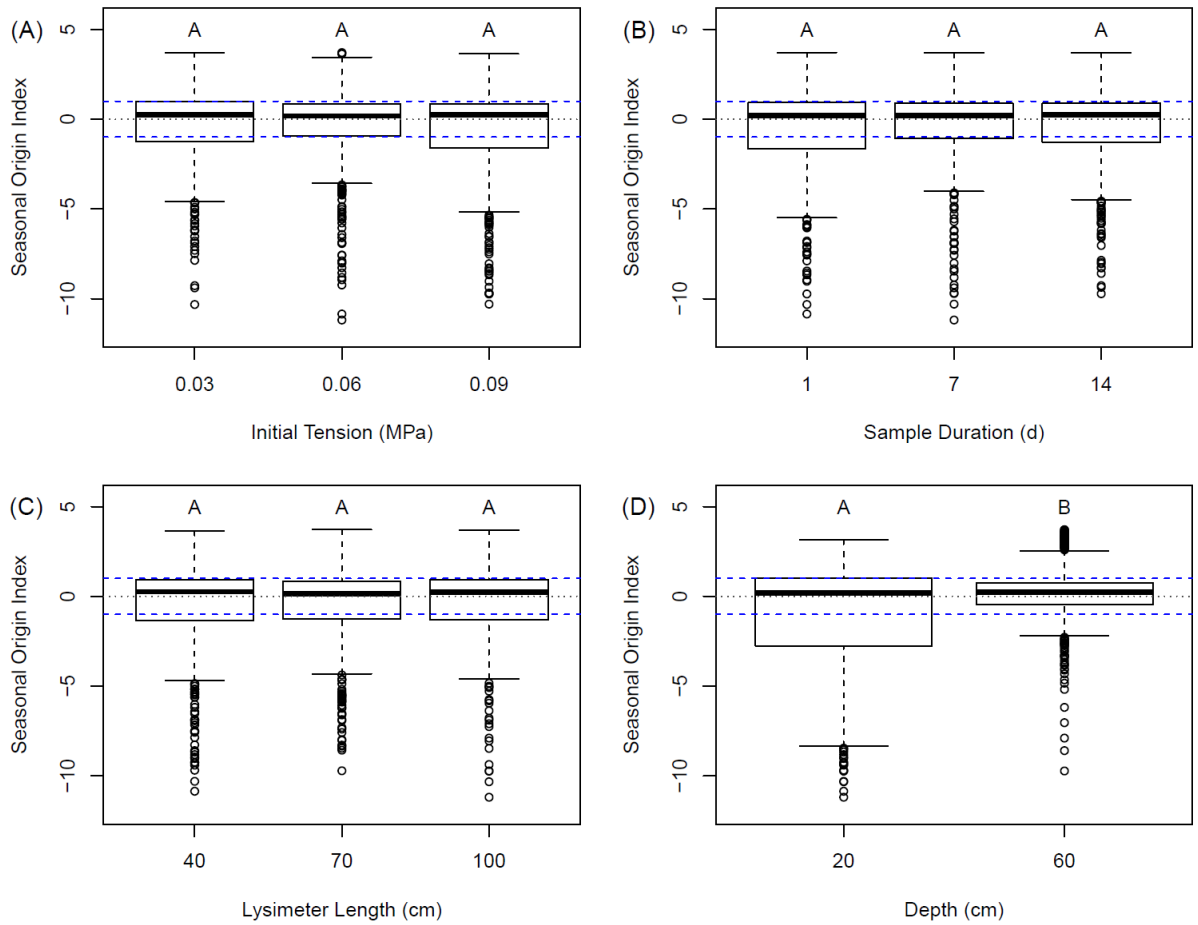

Figure 2.11. Distribution of Seasonal Origin Index by (A) initial lysimeter tension (MPa), (B) sample duration (d), (C) lysimeter length (cm), and (D) lysimeter depth (cm). Samples are marked as outliers (shown as circles) if their value is outside 1.5 times the interquartile range above the upper quartile or below the lower quartile. SOI = ± 1 is marked by blue dashed lines.

6. Water Age

The best-fit cosine and sine coefficients of the annual cycle of precipitation $\delta^{18}O$ were -0.94 and 0.50, respectively, meaning the $\delta^{18}O$ cycle amplitude was 1.07 ‰. The fractions of young water (i.e., water less than 2.3 ± 0.8 months old) in lysimeter samples are reported in Table 2.3. Among all lysimeter samples, young water makes up 58% of total extracted soil water. However, among individual combinations of lysimeter characteristics, young water ranged from 37% to 100% of total extracted soil water.

Lysimeters at 20 cm depth, 40 cm length, sample duration of 1 day, and initial tension of -0.06 MPa had the greatest fractions of young water. Lysimeters at 60 cm depth, 40 cm length, sample duration of 7 days, and initial tension of -0.06 MPa had the smallest fraction of young water. In general, installation depth seemed to have the greatest influence on young water fraction. Lysimeters at 20 cm depth had 96% young water, and lysimeters at 60 cm depth had 57% young water. The fraction of young water did not monotonically increase nor decrease with increasing lysimeter length, sample duration, or initial tension.

Table 2.3. The percentage of young water in lysimeter samples, where young water is defined as water that entered the soil as precipitation within the last 2.3 ± 0.8 months (Kirchner, 2016). Each row corresponds to groupings of lysimeter samples by depth (cm), lysimeter length (LL) (cm), sample duration (SD) (d), and initial tension (- MPa).

Depth (cm)	LL (cm)	SD (d)	Tension (- MPa)	Cosine Coefficient	Sine Coefficient	Amplitude (‰)	% Young Water
All Lysimeter Samples				-0.40	0.47	0.62	57.86
20				-0.97	0.35	1.03	96.53
60				0.17	0.58	0.61	56.89
	40			-0.50	0.52	0.72	67.40
	70			-0.33	0.45	0.56	52.47
	100			-0.36	0.45	0.58	54.10
		1		-0.42	0.55	0.69	64.99
		7		-0.40	0.43	0.58	54.78
		14		-0.37	0.46	0.59	55.04
			0.03	-0.41	0.52	0.66	61.84
			0.06	-0.28	0.44	0.52	48.94
			0.09	-0.50	0.48	0.69	64.68
20	40	1	0.03	-1.17	0.77	1.40	100.00
20	40	1	0.06	-1.46	0.39	1.51	100.00
20	40	1	0.09	-1.22	0.57	1.34	100.00
20	40	7	0.03	-1.06	0.74	1.29	100.00
20	40	7	0.06	-1.12	0.25	1.14	100.00
20	40	7	0.09	-1.23	0.56	1.35	100.00
20	40	14	0.03	-0.83	0.35	0.90	84.55
20	40	14	0.06	-0.61	0.50	0.79	73.92
20	40	14	0.09	-1.01	0.14	1.02	95.47
20	70	1	0.03	-0.57	0.53	0.78	72.95
20	70	1	0.06	-1.13	-0.02	1.13	100.00
20	70	1	0.09	-1.42	0.09	1.43	100.00
20	70	7	0.03	-1.07	0.38	1.14	100.00
20	70	7	0.06	-0.86	0.99	1.32	100.00

Table 2.3 (continued).

20	70	7	0.09	-0.96	0.57	1.11	100.00
20	70	14	0.03	-0.45	0.40	0.60	56.43
20	70	14	0.06	-0.67	0.24	0.71	66.78
20	70	14	0.09	-0.89	0.13	0.90	84.06
20	100	1	0.03	-0.45	0.40	0.60	56.43
20	100	1	0.06	-0.67	0.24	0.71	66.78
20	100	1	0.09	-0.89	0.13	0.90	84.06
20	100	7	0.03	-1.07	0.38	1.14	100.00
20	100	7	0.06	-0.86	0.99	1.32	100.00
20	100	7	0.09	-0.96	0.57	1.11	100.00
20	100	14	0.03	-0.45	0.40	0.60	56.43
20	100	14	0.06	-0.67	0.24	0.71	66.78
20	100	14	0.09	-0.89	0.13	0.90	84.06
60	40	1	0.03	0.25	0.79	0.83	77.54
60	40	1	0.06	0.36	0.63	0.73	68.37
60	40	1	0.09	0.38	0.76	0.85	79.53
60	40	7	0.03	-0.20	0.89	0.91	85.65
60	40	7	0.06	0.14	0.36	0.39	36.67
60	40	7	0.09	0.20	0.49	0.53	49.24
60	40	14	0.03	0.09	0.64	0.64	60.16
60	40	14	0.06	0.17	0.61	0.63	59.36
60	40	14	0.09	-0.63	0.75	0.98	91.95
60	70	1	0.03	0.04	0.50	0.50	46.79
60	70	1	0.06	0.49	0.57	0.75	70.21
60	70	1	0.09	0.26	0.79	0.83	77.79
60	70	7	0.03	0.16	0.65	0.66	62.31
60	70	7	0.06	0.20	0.42	0.46	43.19
60	70	7	0.09	0.31	0.36	0.47	44.51
60	70	14	0.03	0.07	0.42	0.43	40.30
60	70	14	0.06	0.31	0.85	0.91	85.20
60	70	14	0.09	0.02	0.57	0.57	53.56
60	100	1	0.03	0.11	0.69	0.70	65.25
60	100	1	0.06	0.21	0.76	0.79	74.36
60	100	1	0.09	0.31	0.72	0.78	73.45
60	100	7	0.03	0.16	0.43	0.46	43.31
60	100	7	0.06	0.18	0.40	0.44	41.06
60	100	7	0.09	0.25	0.51	0.57	53.23
60	100	14	0.03	0.38	0.48	0.62	57.83
60	100	14	0.06	0.47	0.52	0.70	65.78
60	100	14	0.09	-0.16	0.65	0.67	62.51

Discussion

1. Sample Volume

Lysimeters characteristics strongly influenced sample volume, which increased with increasing initial tension, sample duration, and lysimeter length. These findings are unsurprising because higher tensions pull more water out of the soil, longer sample durations allow more time for the water to be extracted, and longer lysimeter lengths allow more water to be collected due to greater lysimeter volume. At the time of sample collection, the residual vacuum was significantly higher in longer lysimeters ($p < 0.001$), indicating that long lysimeters can maintain greater vacuum power over time. Tension had the greatest influence on sample volume; on average, lysimeters with -0.09 MPa initial tension were three times greater than samples with -0.03 MPa initial tension. Because the applied tension decreases over time, we observe diminishing returns on sample volume with increasing sample duration. Increasing length from 40 to 70 cm allowed larger samples to be collected, increasing the maximum capacity from approximately 725 to 1,270 mL, but the increase from 70 to 100 cm was less critical because most samples were not large enough to require more than 1,270 mL of storage space. The lysimeter cup depth had little influence on sample volume. Although soil water content differed greatly between 20 cm and 60 cm depth in the fall (Figure 2.3c), we observe indistinguishable distributions of sample volumes likely due to low sample yield (48%) caused by dry conditions during this time. Soil water content was similar at low tensions for both depths (Figure 2.4), so these results indicate that soil water at both depths typically experienced tensions lower than the initial applied tension.

Previous research indicates that no meaningful relationship exists between the amount of soil water extracted and freely percolating soil water (van der Ploeg & Beese, 1977), so

implications of these findings are focused on efficient and effective experimental design of lysimeters. Literature suggests that the smallest possible tension and sample duration be applied to achieve the required sample volume to minimize the impact on the natural percolation front (Nash and Leslie, 1991; Severson and Grigal, 1976; Weihermüller, 2005). Soils in this study were sandy loams, so it should be noted that soils with finer textures may require significantly longer than one day to achieve adequate sample volume (Barbee & Brown, 1986; Hansen & Harris, 1975). However, if samples are to be analyzed for nutrients, one should consider that nitrogen transformation and may occur inside the lysimeter if samples are allowed to remain inside for more than approximately two days (Hansen & Harris, 1975). If soil texture prevents rapid collection of samples, then alternative collection methods should be considered (Nash and Leslie, 1991). If samples are to be analyzed for pesticides, minimal tension should be applied to prevent volatilization within the lysimeter (U.S. Environmental Protection Agency, 1982). In summary, lysimeters characteristics should be chosen to balance the required sample volume with chemical properties.

Lysimeter sample volume remained fairly consistent throughout the year of 2013 except for August through November. During these months, sample volumes were limited by low precipitation and dry soils (Figure 2.3b). This variability in sample volume supports concerns in the literature that many lysimeter studies do not collect enough samples or replicates to capture both wet and dry soil water content regimes (Angle et al., 1991). Most studies do not have the resources to install as many lysimeters as used here, so this study highlights the need to carefully consider the number of required lysimeters to fully capture soil water variability (Gomez, 1984) as well as the key characteristics of initial applied tension, sample duration, and lysimeter length. Seasonal variability should also be considered when designing a lysimeter experiment, especially

when few samples will be collected. For future isotope analysis in this particular system (i.e. Chapter 3), we found it sufficient to use lysimeters of 70 cm length, applied tension of -0.06 MPa, and sample durations of 1 day at both depths, 20 and 60 cm.

2. Isotope Composition

Though they influenced sample volume significantly, initial tension, sample duration, and lysimeter length had no significant influence on the isotope composition of lysimeter samples. The fact that sample volume, initial tension, and sample duration affected sample volume by not isotope composition may indicate that the isotope composition of soil at a particular depth (20 and 60 cm) is relatively homogeneous at each point in time. Depth and season were the main drivers of lysimeter sample δ^2H and $\delta^{18}O$ variability. Excluding February, soil water δ^2H and $\delta^{18}O$ exhibited expected sine-wave behavior over the year (Allen, 2016; Kirchner, 2016), with isotopically lighter samples in cooler months and isotopically heavier samples in warmer months (Figure 2.8). However, soil water at 20 cm displayed this sine-wave more strongly than soil water at 60 cm, which remained relatively constant and isotopically heavier at an average of -5.35‰ $\delta^{18}O$ and -28.95‰ δ^2H. These results suggest that the two lysimeter depths sampled relatively distinct pools of water with hydrologic characteristics that evolve through time and reflect new inputs of precipitation and mixing of existing soil water.

The soil water regime indicated by these results can be described by convective-dispersive flow (Vereecken et al., 2016), where pre-existing soil water is displaced imperfectly by precipitation. This type of flow suggests there may be some evidence of "two water worlds," a compartmentalized ecohydrological system where soil water is not fully mixed (Brooks et al., 2010; McDonnell et al., 2014). Similar to findings by Gazis & Feng (2004), deeper soil water appeared to have a longer residence time than shallower soilt water and was only replaced during

substantial rain events, like the large storm on January 30, 2013. Characterizing soil water isotope composition is key to improving models of soil water dynamics in the unsaturated zone and to better understand plant water sources (Bowen, 2015; Gazis & Feng, 2004).

3. Seasonal Origins of Soil Water

According to the SOI, about one third of soil water samples originated in winter, one third originated in summer, and one third represented a mixture of water from all seasons. Different seasons had significantly different distributions of SOI. Summer SOI values still indicate the presence of winter precipitation in summer soils, suggesting that residence times for precipitation are at least several months and suggesting that summer precipitation may flow preferentially through the watershed. In contrast, with the exception of February, winter SOI indicates that soil water is dominated by recent, winter precipitation. The distribution of summer SOI is similar to those found in Switzerland by Allen et al. (2019), despite having a larger seasonal precipitation isotope cycle. Many months included SOI greater 1 and less than -1, beyond the expected SOI limits. These extreme values demonstrate the limitation of the method in regions such as the southern Appalachian Mountains, where isotopic variability of precipitation can be greater between storms than between seasons. Being a new method, these limitations of the SOI have not been discussed elsewhere in the literature.

The SOI values different significantly among the two soil depths, where shallow samples were skewed towards lower SOI with precipitation from winter. These results suggest that deep soil water is a more thorough mix of summer and winter precipitation than shallow soil water, which is removed by growing season evapotranspiration and replenished by recent precipitation. This finding differs from that of Allen et al. (2019), who found that deep soil water was more

likely to reflect winter precipitation than shallow soil water. This difference likely exists because Allen et al. (2019) only examined SOI during one summer season.

4. Soil Water Age

Young water made up 58% of all mobile soil water, 96% of shallow soil water, and 57% of deep soil water. These young water fraction results corroborate the SOI results and provide insight into specific water ages, unlike the coarse scale of the SOI. These relatively high fractions of young water are typical for humid catchments with low storage capacity (von Freyberg et al., 2018). Simulations of forested long-term experimental sites in northern latitudes found similar results with soil water averaging around 75 days (about 2.5 months), ranging from a few days to 300 days over several years (Sprenger, 2018). Most studies have applied the young water fraction to stream water isotopes rather than soil water, and our soil water was consistently younger than stream young water fractions in the literature (e.g., Jasechko et al., 2016; Song et al., 2016).

Depth seemed to have the greatest impact on soil water age; the influences of initial tension, sample duration, and lysimeter length were unclear. Therefore, it is important to sample at multiple soil depths when evaluating young water fractions for soil profiles. The prevalence of young soil water in this ecosystem means that a sampling regime should include frequent sampling throughout the year to fully capture soil water isotopes, particularly within the root zone. These results have implications for not only lysimeter experimental design but also plant water uptake. Imagining trees as lysimeters, we find that trees may be vulnerable to drought if they are more shallowly rooted and rely on young water.

5. Limitations and Future Work

This lysimeter experiment has several limitations due to the nature of lysimeter sampling and the specific setting. Lysimeters collect mobile water that is known to reflect infiltrating precipitation, excluding bulk water that exhibits an evaporation signal (Brooks et al., 2010). By excluding bulk water, which includes both mobile and tightly held waters, from our analysis, we cannot fully explain soil water dynamics and must limit our interpretations to the faster flow domain. If future studies hope to more completely explain soil water dynamics, they should include bulk water sampling methods, such as cryogenic vacuum extraction or direct equilibration (Sprenger et al., 2015). Additionally, depth to groundwater level not recorded, and no groundwater samples were collected in 2013, so we do not know the extent of groundwater mixing in the unsaturated zone, a likely occurrence in the flat, riparian setting. Finally, the soils at this study site were sandy loams and our results may not be applicable to other soil types. Previous work has observed differing fractions of mobile and immobile soil water for other soil textures (Landon et al., 1999), so future work could explore diverse soil textures.

This study aimed to evaluate the annual variability of soil water isotope composition. However, precipitation at Coweeta Hydrologic Laboratory was unique in 2013—it was the second wettest year on record and included the all-time January precipitation record. Given the unusual precipitation quantity and patterns, it may be difficult to generalize our results to typical years. Much of the January precipitation can be attributed to a 13.92 cm storm on January 30 that originated from the Gulf of Mexico and was isotopically heavy. The effect of this event is clearly visible in the soil isotope record for February (Figure 2.8), but no precipitation samples were captured due to failed collectors during the storm. Because the SOI and young water fraction rely

on strong seasonal variations in isotope composition, new methods may be needed for regions where short-term, inter-storm variability can be higher than seasonal variability.

Conclusion

To examine the effects of lysimeter characteristics on sample volume and isotope composition ($\delta^{18}O$ and $\delta^{2}H$), we assessed results from an array of falling-tension lysimeters with multiple lysimeter lengths, tensions, sample durations, and installation depths. We also evaluated seasonal origin and fraction of young water in the unsaturated zone. We found that most lysimeters produced ample volume for typical soil water analyses. Sample volume was largest in the spring and smallest in the dry fall months. Distributions of sample volume were significantly different for each season. Strong temporal dynamics in soil water content indicates that seasonal variability should be considered when designing a lysimeter experiment. Sample volume increased with initial tension, sample duration, and lysimeter length. However, installation depth of sampling cup did not significantly influence sample volume. Initial tension, sample duration, and lysimeter length should be chosen carefully to collect the volume required for analysis while also maintaining the integrity of the sample.

Conversely, initial tension, sample duration, and lysimeter length did not significantly influence the isotope composition of lysimeter samples. Season and depth were the primary drivers of lysimeter sample $\delta^{2}H$ and $\delta^{18}O$ values. Summer soil water was isotopically heavy with minimal variability, and winter soil water was isotopically light with greater variability. Distributions of sample isotope composition were significantly different for each season. Deeper soil water was isotopically lighter and experiences less variability than shallow water. Our findings suggest that the two lysimeter installation depths sample distinct pools of water whose

physical characteristics evolve through time and reflect new inputs of precipitation and mixing of existing soil water, supporting the “two water worlds” hypothesis (Brooks et al., 2010). Furthermore, SOI revealed that one third of soil water samples originated in winter, one third originated in summer, and one third represented a mixture of water from all seasons. Summer soil water indicated the presence of winter precipitation, suggesting a residence time of winter precipitation of several months. This finding was corroborated by water age calculations—58% of all lysimeter water entered the soil as precipitations within the last 2.3 ± 0.8 months. Young water comprised 96% of shallow soil water and 57% of deep soil water. Though specific lysimeter installation methods may not heavily influence the isotope composition of samples, these results may have importance in the context of plant water uptake by rooting depth.

REFERENCES

Akaike, H. (1974). A new look at the statistical model identification. *IEEE Transactions on Automatic Control*, *19*(6), 716–723. doi:10.1109/TAC.1974.1100705.

Allen, S. T., Kirchner, J. W., Braun, S., Siegwolf, R. T., & Goldsmith, G. R. (2019). Seasonal origins of soil water used by trees. *Hydrology and Earth System Sciences Discussions*. doi:10.5194/hess-2018-554.

Allen, S. T., Kirchner, J. W., & Goldsmith, G. R. (2018). Predicting Spatial Patterns in Precipitation Isotope (δ2H and δ18O) Seasonality Using Sinusoidal Isoscapes. *Geophysical Research Letters*, *45*, 4859–4868. doi:10.1029/2018GL077458.

Angle, J. S., McIntosh, M. S., & Hill, R. L. (1991). Tension Lysimeters for Collecting Soil Percolate. In *Groundwater Residue Sampling Design* (pp. 290–299). American Chemical Society. doi:10.1021/bk-1991-0465.ch018.

Austin, A. T., Yahdjian, L., Stark, J. M., Benlap, J., Porporato, A., & Norton, U., et al. (2004). Water pulses and biogeochemical cycles in arid and semiarid ecosystems. *Oecologia*, *141*(2), 221–235. doi:10.1007/s00442-004-1519-1.

Barbee, G. C., & Brown, K. W. (1986). Comparison Between Suction and Free-Drainage Soil Solution Samplers. *Soil Science*, *141*(2), 149–154. doi:10.1097/00010694-198602000-00008.

Barber, S. A. (1995). *Soil nutrient bioavailability: a mechanistic approach*. New York: John Wiley and Sons.

Barnes, C. J., & Turner, J. V. (1998). Isotopic exchange effects in soil water. In C. Kendall & J. McDonnell (Eds.), *Isotope Tracers in Catchment Hydrology* (pp. 137–163). Amsterdam: Elsevier Science.

Benettin, P., Volkmann, T. H. M., von Freyberg, J., Frentress, J., Penna, D., Dawson, T. E., et al. (2018). Effects of climatic seasonality on the isotopic composition of evaporating soil waters. *Hydrology and Earth System Sciences 22*(5), 2881-2890. doi: 10.5194/hess-22-2881-2018.

Briggs, L. J., & McCall, A. G. (1904). An artificial root for inducing capillary movement of soil moisture. *Science*, *20*(5), 566–569. doi:10.1126/science.20.513.566.

Botter, G., Bertuzzo, E., & Rinaldo, A. (2011). Catchment residence and travel time distributions: The master equation. *Geophysical Research Letters*. doi:10.1029/2011gl047666.

Bowen, G. (2015). The diversified economics of soil water. *Nature*, *525*, 43–44. doi:10.1038/525043a.

Brooks, J. R., Barnard, H. R., Coulombe, R., & McDonnell, J. J. (2010). Ecohydrologic separation of water between trees and streams in a Mediterranean climate. *Nature Geoscience*, *3*(2), 100–104. doi:10.1038/NGEO722.

Casey, F. X. M., Derby, N. E., Knighton, R. E., Steele, D. D., & Stegman, E. C. (2002). Initiation of Irrigation Effects on Temporal Nitrate Leaching. *Vadose Zone Journal*, *1*, 300–309. doi:10.2113/1.2.300.

Chorover, J., Kretzschmar, R., Garcia-Pichel, F., & Sparks, D. L. (2007). Soil Biogeochemical Processes within the Critical Zone. *Elements*, *3*(5). doi:10.2113/gselements.3.5.321.

Clark, I. D., & Fritz, P. (1997). *Environmental Isotopes in Hydrogeology*. Boca Raton, FL: CRC Press/Lewis Publishers.

Corwin, D. L. (2002). Suction cups. In J. Dane & G. Topp (Eds.), *In Methods of soil analysis, Part 4, Physical methods* (pp. 1261–1266). Madison, WI: Soil Science Society of America.

Cowan, I. R. (1965). Transport of Water in the Soil-Plant-Atmosphere System. *Journal of Applied Ecology*, *2*(1), 221–239. doi:10.2307/2401706.

Douglass, J. E. (1988). Climatology and hydrology. In W. Swank & D. Crossley, Jr. (Eds.), *Forest hydrology and ecology at Coweeta* (pp. 35–55). New York: Springer-Verlag.

Fares, A., Deb, S. K., & Fares, S. (2009). Review of vadose zone soil solution sampling techniques. *Environmental Reviews*, *17*, 215–234. doi:10.1139/A09-010.

Fetter, C. W. (2001). Soil Moisture and Ground-Water Recharge. In *Applied Hydrogeology, Fourth Edition*. Upper Saddle River, NJ: Prentice-Hall, Inc.

Gardner, W. R. (1960). Dynamic aspects of water availability to plants. *Soil Science*, *89*(2), 63–73. doi:10.1146/annurev.pp.16.060165.001543.

Gazis, C., & Feng, X. (2004). A stable isotope study of soil water: evidence for mixing and preferential flow paths. *Geoderma*, *119*(1-2), 97–111. doi:10.1016/S0016-7061(03)00243-X.

Gomez, K. A., & Gomez, A. A. (1984). *Statistical procedures for agricultural research*. New York: John Wiley and Sons.

Hansen, E. A., & Harris, A. R. (1975). Validity of Soil-Water Samples Collected with Porous Ceramic Cups. *Soil Science Society of America Journal*, *39*(3), 528–536. doi:10.2136/sssaj1975.03615995003900030041x.

Hrachowitz, M., Savenije, H., Bogaard, T. A., Tetzlaff, D., & Soulsby, C. (2013). What can flux tracking teach us about water age distribution patterns and their temporal dynamics? *Hydrology and Earth System Sciences*, *17*, 533–564. doi:10.5194/hess-17-533-2013.

Jasechko, S., Kirchner, J. W., Welker, J. M., & McDonnell, J. J. (2016). Substantial proportion of global streamflow less than three months old. *Nature Geoscience*, *9*(2), 126–129. doi:10.1038/ngeo2636.

Kirchner, J. W. (2016). Aggregation in environmental systems – Part 1: Seasonal tracer cycles quantify young water fractions, but not mean transit times, in spatially heterogeneous catchments. *Hydrology and Earth System Sciences*, *20*(1), 279–297. doi:10.5194/hess-20-279-2016.

Kramer, P. J. (1969). In *Plant & soil water relationships; a modern synthesis*. New York: McGraw-Hill.

Kolenbrander, G. J. (1969). Nitrate content and nitrogen loss in drain water. *Netherlands Journal of Agricultural Science*, *17*, 246–255.

Landon, M. K., Delin, G. N., Komor, S. C., & Regan, C. P. (1999). Comparison of the stable-isotopic composition of soil water collected from suction lysimeters, wick samplers, and cores in a sandy unsaturated zone. *Journal of Hydrology*, *224*(1-2), 45–54. doi:10.1016/S0022-1694(99)00120-1.

Litaor, M. I. (1988). Review of Soil Solution Samplers. *Water Resources Research*, *25*(5), 727–733. doi:10.1029/WR024i005p00727.

McDonnell, J. J. (2014). The two water worlds hypothesis: ecohydrological separation of water between streams and trees? *WIREs Water*, *1*, 323–329. doi:10.1002/wat2.1027.

McDonnell, J. J., McGuire, K., Aggarwal, P., Beven, K. J., Biondi, D., & Destouni, G., et al. (2010). How old is streamwater? Open questions in catchment transit time conceptualization, modelling and analysis. *Hydrological Processes*, *24*, 1745–1754. doi:10.1002/hyp.7796.

Michelsen, N., van Geldern, R., Roßmanna, Y., Bauera, I., Schulz, S., & Barth, J. A. C., et al. (2018). Comparison of precipitation collectors used in isotope hydrology. *Chemical Geology*, *488*, 171–179. doi:10.1016/j.chemgeo.2018.04.032.

Miller, D. E. (1967). Available Water in Soil as Influenced by Extraction of Soil Water by Plants. *Agronomy Journal*, *59*(5), 420–423. doi:10.2134/agronj1967.00021962005900050012x.

Miniat, C.F., Laseter, S.H., Swank, W.T., & Swift Jr., L.W. (2015). Daily air temperature, relative humidity, vapor pressure, PPFD, wind speed and direction for climate stations at the Coweeta Hydrologic Lab, North Carolina. *Forest Service Research Data Archive*. doi:10.2737/RDS-2015-0042.

Miniat, C.F., Laseter, S.H., Swank, W.T., & Vose, J.M. (2016). Daily streamflow data for watersheds at Coweeta Hydrologic Lab, North Carolina. *Forest Service Research Data Archive*. doi:10.2737/RDS-2016-0025.

Miniat, C.F., Laseter, S.H., Swank, W.T., & Swift Jr., L.W. (2017). Daily precipitation data from recording rain gages (RRG) at Coweeta Hydrologic Lab, North Carolina. *Forest Service Research Data Archive*. doi:10.2737/RDS-2017-0031.

National Cooperative Soil Survey (2004). Saunook Series. *Official Soil Series Descriptions*. https://soilseries.sc.egov.usda.gov/OSD_Docs/S/SAUNOOK.html.

Nippgen, F., McGlynn, B.L, Emanuel, R.E., & Vose, J.M. (2016). Watershed memory at the Coweeta Hydrologic Laboratory: The effect of past precipitation and storage on hydrologic response. *Water Resources Research 52*(3), 1673-1695. doi: 10.1002/2015WR018196.

Paramasivam, S., Alva, A. K., & Fares, A. (1997). Vadose zone soil solution sampling techniques to investigate pollutant transport in soils. In *Trends in Soil Science, Volume 2*. Trivandrum: Council of Scientific Integration.

R Core Team (2018). R: A language and environment for statistical computing. R Foundation for Statistical Computing, Vienna, Austria. http://www.R-project.org/.

Ritchie, J. T. (1981). Soil water availability. *Plant and Soil*, *58*(1-3), 327–338. doi:10.1007/BF02180061.

Severson, R. C., & Grigal, D. F. (1976). Soil Solution Concentrations: Effect Of Extraction Time Using Porous Ceramic Cups Under Constant Tension. *Journal of the American Water Resources Association*, *12*(6), 1161–1170. doi:10.1111/j.1752-1688.1976.tb00252.x.

Shiklomanov, I. (1993). World fresh water resources. In P. Gleick (Ed.), *Water in Crisis: A Guide to the World's Fresh Water Resources*. New York: Oxford University Press.

Singh, N.K., Emanuel, R.E., & McGlynn, B.L. (2016). Variability in isotopic composition of base flow in two headwater streams of the southern Appalachians. *Water Resources Research 52*(6), 4264-4279. doi: 10.1002/2015WR018463.

Skopp, J., Jawson, M. D., & Doran, J. W. (1990). Steady-State Aerobic Microbial Activity as a Function of Soil Water Content. *Soil Science Society of America Journal*, *54*(6), 1619–1625. doi:10.2136/sssaj1990.03615995005400060018x.

Soil Survey Staff, Natural Resources Conservation Service, United States Department of Agriculture. (2018, September 11). Web Soil Survey. Retrieved from https://websoilsurvey.sc.egov.usda.gov.

Song, C., Wang, G., Liu, G., Mao, T., Sung, X., Chen, X. (2016). Stable isotope variations of precipitation and streamflow reveal the young water fraction of a permafrost watershed: *Hydrological Processes, 31*(4), 935-947. doi: 10.1002/hyp.11077.

Sprenger, M., Herbstritt, B., & Weiler, M. (2015). Established methods and new opportunities for pore water stable isotope analysis. *Hydrological Processes, 29*(25), 5174–5192. doi:10.1002/hyp.10643.

Sprenger, M., Leistert, H., Gimbel, K., & Weiler, M. (2016). Illuminating hydrological processes at the soil-vegetation-atmosphere interface with water stable isotopes. *Reviews of Geophysics 54*, 674-704. doi: 10.1002/2015RG000515.

Sprenger, M., Tetzlaff, D., Buttle, J., Laudon, H., & Soulsby, C. (2018). Water ages in the critical zone of long-term experimental sites in northern latitudes. *Hydrology and Earth System Sciences, 22*, 3965–3981. doi:10.5194/hess-22-3965-2018.

Stagnitti, F., Villiers, N., Parlange, J.-Y., Steenhuis, T. S., de Rooij, G. H., & Li, L., et al. (2003). Solute and Contaminant Transport in Heterogeneous Soils. *Bulletin of Environmental Contamination and Toxicology*, *71*(4), 737–745. doi:10.1007/s00128-003-0194-y.

Swank, W. T., & Crossley, Jr., D. A. (1988). Introduction and Site Description. In *Forest hydrology and ecology at Coweeta* (pp. 3–16). New York: Springer-Verlag.

Swank, W. T. & J. E. Douglass. (1975). Nutrient flux in undisturbed and manipulated forest ecosystems in the southern Appalachian Mountains., in *Proceedings of the Tokyo Symposium in the Hydrological Characteristics of River Basins,* Int. Assoc. of Hydrol. Sci., Washington, D.C.

Swift Jr., L.W, Cunningham, G.B., & J.E. Douglass. (1988). Climatology and Hydrology. In *Forest hydrology and ecology at Coweeta* (pp. 35–56). New York: Springer-Verlag.

Tanweer, A., M. Groning, M. Van Duren, M. Jaklitsch, and L. Poltenstein (2009), Stable isotope internal laboratory water standards: Preparation, calibration, and storage, International Atomic Energy Agency technical procedure note 43.

Tetzlaff, D., Buttle, J., Carey, S. K., van Huijgevoort, M. H. J., Laudon, H., & McNamara, J., et al. (2015). A preliminary assessment of water partitioning and ecohydrological coupling in northern headwaters using stable isotopes and conceptual runoff models. *Hydrological Processes*, *29*(25), 5153–5173. doi:10.1002/hyp.10515.

Tracy, J. C., & Mariño, M. A. (1989). Solute Movement Through Root-Soil Environment. *Journal of Irrigation and Drainage Engineering*, *115*(4). doi:10.1061/(ASCE)0733-9437(1989)115:4(608).

U.S. Environmental Protection Agency. (1982). Physical/chemical methods. In *Test methods for analysis of solid waste, SW-846 2nd edition*. Washington, D.C.: Office of Solid Waste and Emergency Response.

U.S. Geological Survey. (2009). Coweeta Basin 10m DEM, Coweeta LTER File Archive, University of Georgia, Athens, GA. Retrieved from http://coweeta.uga.edu/dbpublic/resource_details.asp?id=404.

van der Ploeg, R. R., & Beese, F. (1977). Model Calculations for the Extraction of Soil Water by Ceramic Cups and Plates. *Soil Science Society of America Journal*, *41*(3), 466–470. doi:10.2136/sssaj1977.03615995004100030007x.

Vereecken, H., Schnepf, A., Hopmans, J. W., Javaux, M., Or, D., & Roose, T., et al. (2016). Modeling Soil Processes: Review, Key Challenges, and New Perspectives . *Vadose Zone Journal*, *15*(5). doi:10.2136/vzj2015.09.0131.

von Freyberg, J., Allen, S. T., Seeger, S., Weiler, M., & Kirchner, J. W. (2018). Sensitivity of young water fractions to hydro-climatic forcing and landscape properties across 22 Swiss catchments. *Hydrology and Earth System Sciences*, *22*(7), 3841–3861. doi:10.5194/hess-22-3841-2018.

Warrick, A. W., & Amoozegar-Fard, A. (1977). Soil water regimes near porous cup water samplers. *Water Resources Research*, *13*(1), 203–207. doi:10.1029/WR013i001p00203.

Weihermüller, L. (2005). *Comparison of different soil water extraction systems for the prognoses of solute transport at the field scale using numerical simulations* (Doctoral dissertation). Retrieved from http://hdl.handle.net/2128/490.

Weihermüller, L., Siemens, J., Deurer, M., Knoblauch, S., Rupp, H., & Göttlein, A. (2007). In Situ Soil Water Extraction: A Review. *Journal of Environmental Quality*, *36*(6), 1735–1748. doi:10.2134/jeq2007.0218.

CHAPTER 3: Determination of Tree Water Sources and Residence Times Using Stable Isotopes in a Southern Appalachian Forest

Abstract

We expect substantial changes in quantities and patterns of drinking water supply in the face of climate change and population growth. Because 53% of water supply in the United States originates on forested land, forest extent and composition are key components to managing water supplies. Hydrologic models are useful tool to predict changes in hydrological processes and water supply as a result of climate and land use dynamics. Many watershed models simplify biological processes associated with plant water uptake and transpiration, often assuming that roots uptake water from the same moisture pool that feeds the stream. Several studies using the stable isotope of water have suggested that this assumption may be incorrect due to incomplete mixing of subsurface waters. However, tree water use has not been explored using stable isotopes in humid watersheds with low seasonable variability. Here we show that tree water sources and residence times significantly vary by tree species in a humid catchment. We found that *R. maximum*, an evergreen diffuse-porous shrub, used young water that reflects recent precipitation and shallow soil water. In contrast, *Q. alba*, a deciduous ring-porous tree, used older soil water that reflects a mixture of precipitation from multiple seasons. *A. rubrum* and *L. tulipifera*, deciduous diffuse-porous trees, generally sourced water from winter precipitation but used a variety of water sources throughout the year. These results demonstrate that tree species partition water resources within a single site and that ecohydrologic separation is less pronounced at this humid site. Our findings have implications for drought vulnerability and

forest management, as species that rely on young water for transpiration may be more susceptible to dry periods.

Introduction

Climate change and population growth are major challenges to drinking water availability and sustainable water management. We expect changes in the global water cycle to accompany climate warming, as the saturation vapor pressure of water in air is highly sensitive to temperature (Allen & Ingram, 2002). Even small shifts in climate can cause substantial changes in extreme weather events, such as flooding (Knox, 2000) and drought (Seager et al., 2009), affecting quantities and patterns of available drinking water. Furthermore, water infrastructure, particularly in the southeast United States, was developed to fit the historical behavior of the hydroclimate (Milly et al., 2008) and may not be suitable for projected changes in runoff (Luce and Holden, 2009; Rice et al., 2008; Seager et al., 2008). The world's population is expected to increase by an additional one billion people by the year 2030 (United Nations, 2015), further challenging our ability to satisfy both human demand for water and the maintenance of healthy freshwater systems (Postel, 2000).

Forest extent and composition are key components to managing water supplies (Ford et al., 2011b). Approximately 53% of water supply in the coterminous United States originates on forested land, so water runoff and its quality are a major focus of forest management (Brown et al., 2008; Kim et al., 2014). Rising temperatures may increase plant water use via transpiration and evaporation, leaving less water for streamflow and groundwater recharge (Emanuel, 2018). Additionally, forest distribution and species composition are likely to undergo radical changes due to climate warming, including increased wind and ice damage, hurricane intensity, the

spread of invasive pests, late-season drought, and increased fire (Iverson et al., 2008; Brantley et al., 2013). Because different tree species have varying evapotranspiration responses to climatic variables, we must consider plant water use with respect to tree species, size, landscape position, and hydraulic behavior (Ford et al., 2011a).

Hydrologic models are one way to predict changes in hydrological processes and water supply as a result of climate and land use dynamics. A limitation of many hydrologic models is that they simplify biological processes associated with plant water uptake and transpiration. Many watershed models have inferred the mechanisms behind vegetation-streamflow interactions instead of explicitly representing evapotranspiration (Bosch & Hewlett, 1982; Jones, 2000; Jones & Grant, 1996). In particular, hydrologic models often assume that roots take up water from the same moisture pool that feeds the stream, though several studies using stable isotope tracers have suggested that this assumption may be incorrect (e.g., Brooks et al., 2010; Cernusak et al., 2016; Goldsmith et al., 2012).

Stable isotopes of hydrogen and oxygen in water vary based on time, water source, and the movement of water, so examining the ratio of heavy to light isotopes can help discern the age and origin of water (Kendall & McDonnell, 1998). Using stable isotopes, Dawson and Ehleringer (1991) demonstrated complex interactions between plant water and hydrologic pools, showing that some streamside trees used deeper groundwater instead of stream water. Other studies have found that trees do not necessarily take water from the same pool as streams, especially with increasing root depth and during dry conditions (Cernusak et al., 2016). In places with strong climate seasonality, two distinct "water worlds" may emerge during dry seasons: (1) mobile water in streams, and (2) tightly bound soil water found in plant tissues (Brooks et al., 2010). Evaristo (2016) demonstrated the ecohydrological separation between tree-transpired water and

stream water; the groundwater and stream components of the water balance have a water source that is transported quickly to a deeper subsurface storage compared to the waters used by trees. The concept of "two water worlds" and ecohydrologic separation continues to be debated, as others have found no evidence for isotopic separation (Geris et al., 2015), questions its applicability to other climates (McDonnell, 2014), and call for further hypothesis testing (Berry et al., 2018). Nonetheless, the previous, false assumption that subsurface water is completely mixed can no longer be accepted (Brooks et al., 2010), and more research is required to better understand plant water use.

Recent studies have explored the source of water uptake by specific tree species (e.g. Barbeta et al., in review; Matheny et al., 2016; Sprenger et al., 2018; Zhu et al., 2018), but these species are mainly found in semi-arid climates, coastal systems, or northern latitudes. Humid ecosystems represent an important literature gap, as regions with high precipitation play a major role in the regulation of the global hydrologic cycle and are the origination point for many water supply regions.

Several techniques have emerged to quantify these hydrologic fluxes and intra-annual isotopic variability. The Seasonal Origin Index (SOI) describes the season in which lysimeter soil water originated as precipitation (Allen et al., 2019). Similarly, the young water fraction estimates the proportion of soil water that recently entered the unsaturated zone (Kirchner, 2016). However, these new methods have not been widely applied to the tree xylem water pool. Though conceptual framework of ecohydrologic separation has been studied in several climates and geographic regions, further testing is required in diverse regions to gain knowledge about tree water use that can be applied to hydrologic models (Brooks et al., 2010).

This study explores tree water source and residence time in the humid southern Appalachians by using the stable isotopes of water ($\delta^{18}O$ and $\delta^{2}H$). We collected seasonal samples from four water pools—soil water, stream water, groundwater, and precipitation—and four tree species—R*hododendron maximum* (rhododendron), *Acer rubrum* (red maple), *Liriodendron tulipifera* (tulip poplar), and *Quercus alba* (white oak)—for one year. We address the following questions: (a) How does tree water source differ by tree species and landscape position? (b) How does tree water source change seasonally? (c) What is the residence time of water in trees?

Site Description

This study was conducted at Coweeta Hydrologic Laboratory, a U.S. Forest Service Experimental Forest located in the Nantahala Mountain Range of western North Carolina and Blue Ridge physiographic province of the southern Appalachians (latitude 35°03' N, longitude 83°25' W) (Swank & Crossley, 1988). Climate in the Coweeta basin is classified as marine humid temperature due to high moisture and mild temperatures (Swift et al., 1988). The mean annual temperature is 12.6 °C, seasonally ranging from 2.9 °C to 21.8 °C (Miniat et al., 2015). The average growing season extends from early May to early October (Swift et al., 1988). Annual precipitation is abundant, averaging approximately 1,800 mm and comprised of less than 10% snowfall. Precipitation is greatest in the dormant season (Miniat et al., 2017).

Vegetation in the Coweeta basin was traditionally considered of the oak-chestnut type but has been reclassified to the oak-hickory classification due to the chestnut blight. Species composition at low elevations is a mix of deciduous oaks with evergreen shrubs *Rhododendron maximum* and mountain laurel (*Kalmia latifolia*) (Day Jr. et al., 1988). Other common species

include red maple (*Acer rubrum*), tulip poplar (*Liriodendron tulipifera*), black birch (*Betula lenta*), and hickories (*Carya* spp.). The specific area of Coweeta Hydrologic Laboratory that was used for our study has been unmanaged by humans since 1924 (Day Jr. et al., 1988).

Soils in the Coweeta basin are generally deep sandy loams underlain by folded schist and gneiss. Soils in the basin are either immature Inceptisols, found on steep slopes at high elevation, or older developed Ultisols, found on both steep ridges and gentle slopes (Swank & Crossley, 1988). The Saunook soil series, defined by fine-loamy, mixed, superactive, mesic Humic Hapludults, was the most prevalent soil type in the study site at the base of the Coweeta basin (Soil Survey Staff, 2018). These well-drained soils have moderately high to high saturated hydraulic conductivity, moderate permeability, and negligible surface runoff (National Cooperative Soil Survey, 2004). Depth to bedrock is approximately 6 m (Swank and Douglass, 1975), and depth to refusal ranges from 0.9 to 3.5 m below the surface (Singh et al., 2016).

Streamflow is perennial in the small watersheds with low variability in flow throughout the year. Discharge is highest and most variable in winter and low and most stable in fall. Overland flow rarely occurs; runoff ratios are typically less than 0.10 (Swank & Douglass, 1975). Soil water storage is a critical pool at Coweeta, especially in low elevation watersheds, due its strong memory of past precipitation for a period of up to one year (Nippgen et al., 2016). Most precipitation events contribute to unsaturated soil storage or evaporation rather than groundwater, which is relatively stable and only responds to the largest storms (Singh et al., 2018).

Methods

1. Experimental Design

Our study took place at the base of the Coweeta basin on the west-facing slope of a first-order tributary (Figure 3.1). The site spans a 100 m stream reach and is approximately 60 m wide with 40 m of elevation gain. A dense evergreen understory with *Rhododendron maximum* surrounds the stream and is overtopped by a deciduous overstory. This site was chosen due to its proximity to a small stream, flux tower, climate station, and pre-existing infrastructure that facilitated data collection.

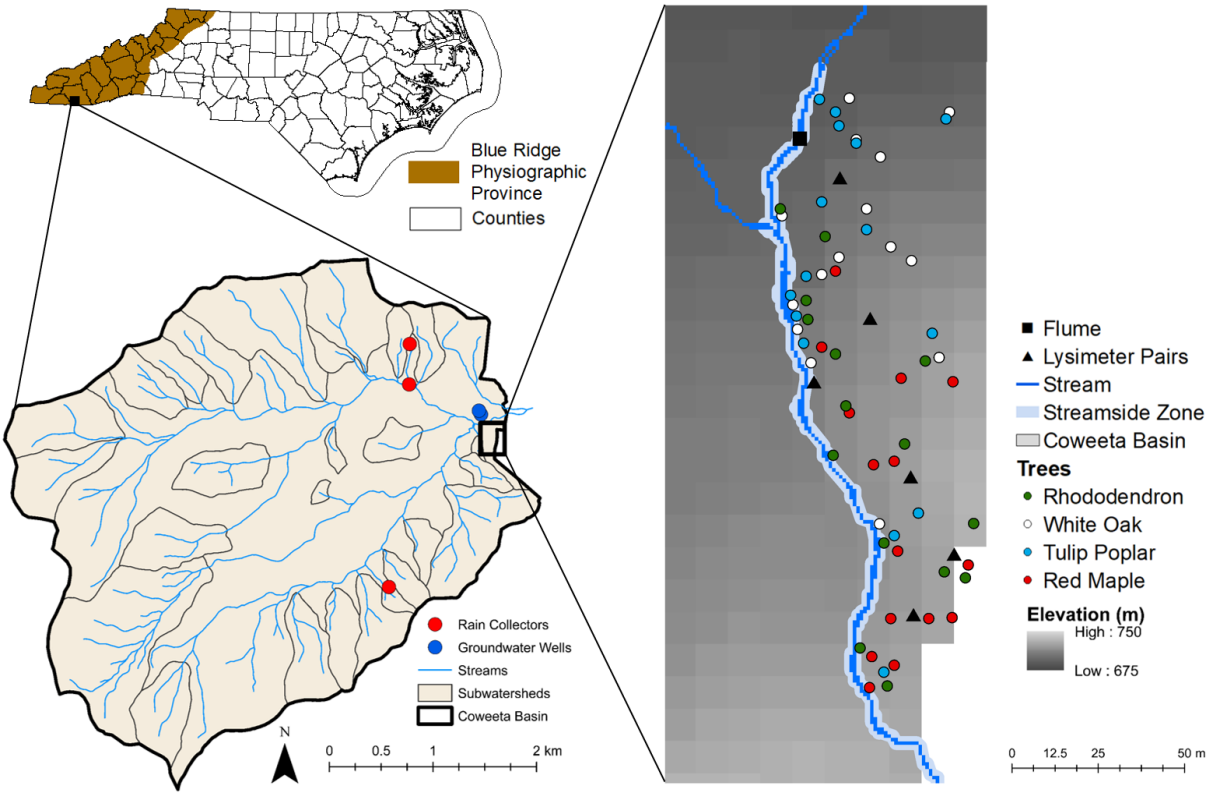

Figure 3.1. Site map at Coweeta Hydrologic Laboratory, North Carolina in the Blue Ridge physiographic province of the southern Appalachian Mountains. The study site (right) was located at the bottom of the Coweeta basin

Seasonal sampling of tree cores, stream water, soil water, and groundwater occurred in 2017 – 2018 and aimed to capture the growing season, the mid-point of fall leaf senescence, the dormant season, the mid-point of spring leaf-on, and an additional growing season. Sampling dates were August 4, 2017, September 2, 2017, October 21, 2017, January 30, 2018, May 2, 2018, June 18, 2018, and August 6, 2018. During site visits, all sampling occurred between precipitation events. Climate, sap flux, soil moisture, and streamflow data were collected continuously. Precipitation samples were collected at least bi-weekly throughout the study period.

Table 3.1. Summary statistics for sampling trees, including species, total number, mean diameter at breast height (DBH) (cm), mean distance to stream (m), mean elevation (m), mean hillslope gradient, and number of trees that were probed for sap flux measurements.

Tree Species	Common Name	Total #	Mean DBH ± SD (cm)	Mean Distance to Stream (m)	Mean Elevation (m)	Mean Gradient
Rhododendron maximum	Rhododendron	15	8.8 ± 1.4	13.1	702	0.19
Acer rubrum	Red maple	15	23.0 ± 15.7	15.4	703	0.28
Liriodendron tulipifera	Tulip poplar	15	31.1 ± 14.1	12.9	717	0.37
Quercus alba	White oak	15	39.3 ± 11.5	17.9	713	0.32

We selected sixty trees for sampling, including fifteen individuals of four different species (Figure 3.1 and Table 3.1). The four species represent two contrasting xylem anatomies—*Rhododendron maximum* (rhododendron), an evergreen diffuse-porous shrub, *Acer rubrum* (red maple), a mid-story diffuse-porous tree, *Liriodendron tulipifera* (tulip poplar), an overstory diffuse-porous tree, and *Quercus alba* (white oak), an overstory ring-porous tree. Trees were selected to span the 100 m stream reach and the full elevation gradient. Three individuals of each species were located within 3 meters of the stream, hereafter referred to as "streamside trees." Diameter at breast height ranged from 8.0 to 65.4 cm. Using an increment borer, a small tree core, approximately 5 mm in diameter and 5 cm in length, was collected from each tree near breast

height (1.3 m above ground) on the upslope side of the tree on each sampling date. The increment borer was cleaned between tree samples. Tree cores were wrapped in parafilm and placed inside a clean 20 mL glass scintillation vial that was sealed tightly, wrapped in parafilm, and placed inside a cooler to prevent evaporation (Dawson, 1993). Tree cores were stored in a freezer in the lab until analyzed for isotopes.

Mobile soil water was collected in six locations that were selected to cover the spatial distribution of sampled trees (Figure 3.1). Pairs of falling-tension lysimeters were installed at 20 and 60 cm at each location. Lysimeters were 70 cm PVC tubes with outside diameter of 4.8 cm capped with two-hole rubber stoppers and epoxied to porous clay cups (Soilmoisture Equipment Corp., Santa Barbara, USA). Teflon tubing in the stopper and Nalgene plastic tubing inside the PVC tubing permitted vacuum application and sample extraction. An initial tension of -0.06 MPa was applied to each lysimeter, and samples were collected by hand pump 24 hours later into 20 mL glass vials sealed with a cone top cap to eliminate headspace and avoid isotopic fractionation. If samples were smaller than 20 mL, glass beads were added to the vial to reduce headspace.

Stream water was collected in thirteen locations along the stream reach. Twelve samples were collected adjacent to each streamside tree. One sample was collected at the flume at the end of the stream reach on the north end of the study site. Stream water was collected by grab sample using 20 mL glass vials sealed with cone top caps to eliminate headspace and avoid isotopic fractionation. Groundwater was collected from two wells, depths 6.7 and 88.7 m, located 200 m northeast of the study site. Samples was collected with bailers and also stored in 20 mL glass vials sealed with cone top caps to eliminate headspace and avoid isotopic fractionation. Groundwater was collected on every sampling date except the first, August 4, 2017.

We collected precipitation samples in bulk collectors distributed throughout the Coweeta basin. Collectors were constructed from 10 cm diameter polycarbonate rain gauges with a thin (5-10 mm) layer of mineral oil inside to prevent evaporation (Michelsen et al., 2018). Water samples were collected using a clean, dry polyethylene syringe and tubing to extract water from beneath mineral oil. We transferred water from the syringe into a 20 mL high-density polyethylene (HDPE) vials sealed with a cone top cap. After sampling, precipitation collectors were cleaned and dried, and new mineral oil was added. Precipitation samples were collected every 1-4 weeks, depending on the total amount of precipitation. Total liquid water depth in the collector at the time of sampling was used to compute volume-weighted averages of precipitation oxygen and hydrogen isotopes for each week. All precipitation isotopes are reported in volume-weighted values. Frozen precipitation occurred infrequently and was not included in this study.

We obtained daily precipitation, temperature, and relative humidity from a nearby long-term climate station (Climate Station 01, latitude 35.07382, longitude -83.47845) located approximately 300 m from the study site at similar elevation. We measured streamflow at the flume at five-minute intervals using a pressure transducer (Model CS-450, Campbell Scientific, Logan, UT). We monitored soil water content using pairs of time-domain reflectometer (TDR) probes installed at 0-30 cm and 30-60 cm depths. Four pairs were placed along a hillslope transect in the middle of the study site. Observations from the probes were recorded at 15-minute intervals using a datalogger (Model CS-625, Campbell Scientific, Logan, UT).

2. Isotope Analysis

All soil water, stream, groundwater, and precipitation samples were stored in a cool place until analyzed in the lab. At the time of analysis, samples were transferred to 2 mL glass vials and

analyzed for $\delta^{18}O$ and $\delta^{2}H$ using a cavity ring-down laser spectrometer (model L2120-*i*, Picarro Inc., Santa Clara, CA, USA, ±0.05 ‰) equipped with an HTC PAL autosampler (LEAP Technologies, Inc., Carrboro, NC, USA). Isotope compositions ($\delta^{18}O$ and $\delta^{2}H$) were reported in per mil (‰) relative to a standard as

$$\delta^{18}\mathrm{O} \text{ or } \delta^{2}\mathrm{H} = \left(\frac{R_{sample}}{R_{standard}} - 1\right) * 1000 \quad (1)$$

where *R* is the ratio of ^{2}H to ^{1}H atoms or ^{18}O to ^{16}O atoms of the sample and the lab standard. Internal lab standards were calibrated against International Atomic Energy Agency (IAEA) standards Vienna Standard Mean Ocean Water (VSMOW2, 0 ‰ $\delta^{18}O$ and 0 ‰ $\delta^{2}H$), Greenland Ice Sheet Precipitation (GISP, -24.76 ‰ $\delta^{18}O$ and -189.5 ‰ $\delta^{2}H$), and Standard Light Antarctic Precipitation (SLAP2, -55.50 ‰ $\delta^{18}O$ and -427.5 ‰ $\delta^{2}H$). Isotope compositions are also reported as deuterium excess to identify vapor source regions, defined as

$$\mathrm{d} = \delta^{2}\mathrm{H} - 8 \times \delta^{18}\mathrm{O} \quad (2)$$

To analyze tree xylem water, we used a Picarro Induction Module (IM) to inductively heat the tree core samples and deliver water vapor to a cavity ring-down laser spectrometer (model L2120-*i*, Picarro Inc., Santa Clara, CA, USA, ±0.05 ‰). Dry air (< 2 ppm H_2O) was delivered via a compressed air tank. We flushed vials with dry air prior to inserting thin, approximately 1 mm, slices of frozen tree cores held inside a folded metal sample hold. We analyzed two blanks prior to each sequence of standards and samples. Liquid internal lab standards were pipetted onto filter paper and were run at the beginning and end of each sequence of samples. We used the "Calibration – High Temperature" recipe and the "Woody Stem" recipe, both supplied by Picarro, to analyze standards and samples, respectively. Due to time constraints, 200 out of 420 total tree cores were analyzed—ten tree cores per species across five sampling dates.

Raw instrument data were corrected in MATLAB (R2018a, Mathworks, Inc., Natick, MA, USA) according to guidelines published by the IAEA Isotope Hydrology Laboratory (Tanweer et al., 2009). Instrument δ^2H accuracy was 0.95 ‰ and precision was 0.21 ‰, giving a total instrument δ^2H uncertainty of 1.17 ‰. Instrument $\delta^{18}O$ accuracy was 0.05 ‰ and precision was 0.05 ‰, resulting in total instrument $\delta^{18}O$ uncertainty of 0.10 ‰.

We used the SOI, developed by Allen et al. (2019), to characterize when lysimeter soil water originated as precipitation. SOI is defined as

$$\mathrm{SOI} = \begin{cases} \dfrac{\delta_x - \delta_{annP}}{\delta_{summerP} - \delta_{annP}}, \text{if } \delta_x > \delta_{annP} \\ \dfrac{\delta_x - \delta_{annP}}{\delta_{annP} - \delta_{winterP}}, \text{if } \delta_x < \delta_{annP} \end{cases} \quad (3)$$

where δ_x is the fractionation-compensated δ^2H isotopic signature of lysimeter soil water samples, and $\delta_{winterP}$, $\delta_{summerP}$, and δ_{annP} are the δ^2H isotopic signatures of typical winter, typical summer, and volume-weighted annual precipitation. We used iteratively reweighted least squares multiple regression on lysimeter sample δ^2H to calculate a measure of central tendency (*offset*) and strength of seasonal cycle (*amplitude*). Typical winter precipitation was defined as $\delta_{winterP}$ = *offset* – *amplitude*, and typical summer precipitation was defined as $\delta_{summerP}$ = *offset* + *amplitude*. To compensate for fractionation effects of δ_x, soil isotope values were adjusted back to the LMWL along an evaporation line slope, calculated by the Craig-Gordon model for diffusion-controlled soil evaporation scenarios by Bennetin et al. (2018). The SOI is near -1.0 for water samples derived entirely from winter precipitation, near 1.0 for sample derived entirely from summer precipitation, and near 0 if they represent a mixture of waters from all seasons. The SOI may exceed the bounds of -1 to 1 if intra-season variability is greater than inter-seasonal variability; a winter sample, for example, may be isotopically lighter than typical winter precipitation and have an SOI less than -1. This method differs from a simple, two-end member mixing model because it accounts for

seasonal rainfall patterns; for example, we may expect to see more winter water than summer water in the soil if precipitation is greater in winter.

To further describe water age, we used the fraction of young water, described by Kirchner (2016), to quantify the percentage of soil water that entered the unsaturated zone as precipitation in the last 2.3 ± 0.8 months. The basis of the young water fraction methods is the seasonal cycles of $\delta^{18}O$ in precipitation and soil water. We used cosine and sine waves to fit our precipitation and soil water data to seasonal cycle curves. Cosine and sine coefficients were calculated for soil water and precipitation by iteratively reweighted least squares multiple regression on $\delta^{18}O$ values for weekly depth-weighted precipitation and groups of lysimeter samples. The amplitude of each cycle was calculated by taking the square root of the sum of the squares of the cycle coefficients. The percentage of young water for each group of lysimeter samples was calculated by dividing the lysimeter $\delta^{18}O$ cycle amplitude by the precipitation $\delta^{18}O$ cycle amplitude and multiplying by 100. Young water percentages may be over 100% if the precipitation isotope record does not fully capture its variability. Young water percentage was capped at 100% in this study.

3. Statistical Analysis

All data processing and statistical analyses were performed in R (R Core Team, 2018). Samples were excluded from isotope analysis if they were deemed outliers by Chauvenet's criterion or if lab notes indicated that the sample had evaporated due to vial headspace or broken vials. We used the "lm" function to perform linear regression. We used the "kruskal.test" function to use the Kruskal-Wallis Test to compare medians and distributions of sample volume, isotope composition, SOI, and young water fraction. We used the "posthoc.kruskal.nemenyi.test" function as a post-hoc test to calculate pairwise multiple comparisons between group levels.

Results

1. Hydrologic Conditions

During the study period of August 2017 – August 2018, mean daily temperature was 14.6 °C, ranging from -9.4 °C in January to 25.8 °C in July (Figure 3.2a). Mean monthly temperatures were typical of long-term records apart from February 2018 at 10.0 °C, 115% warmer than average, and January 2018 at 1.0 °C, 65% colder than average.

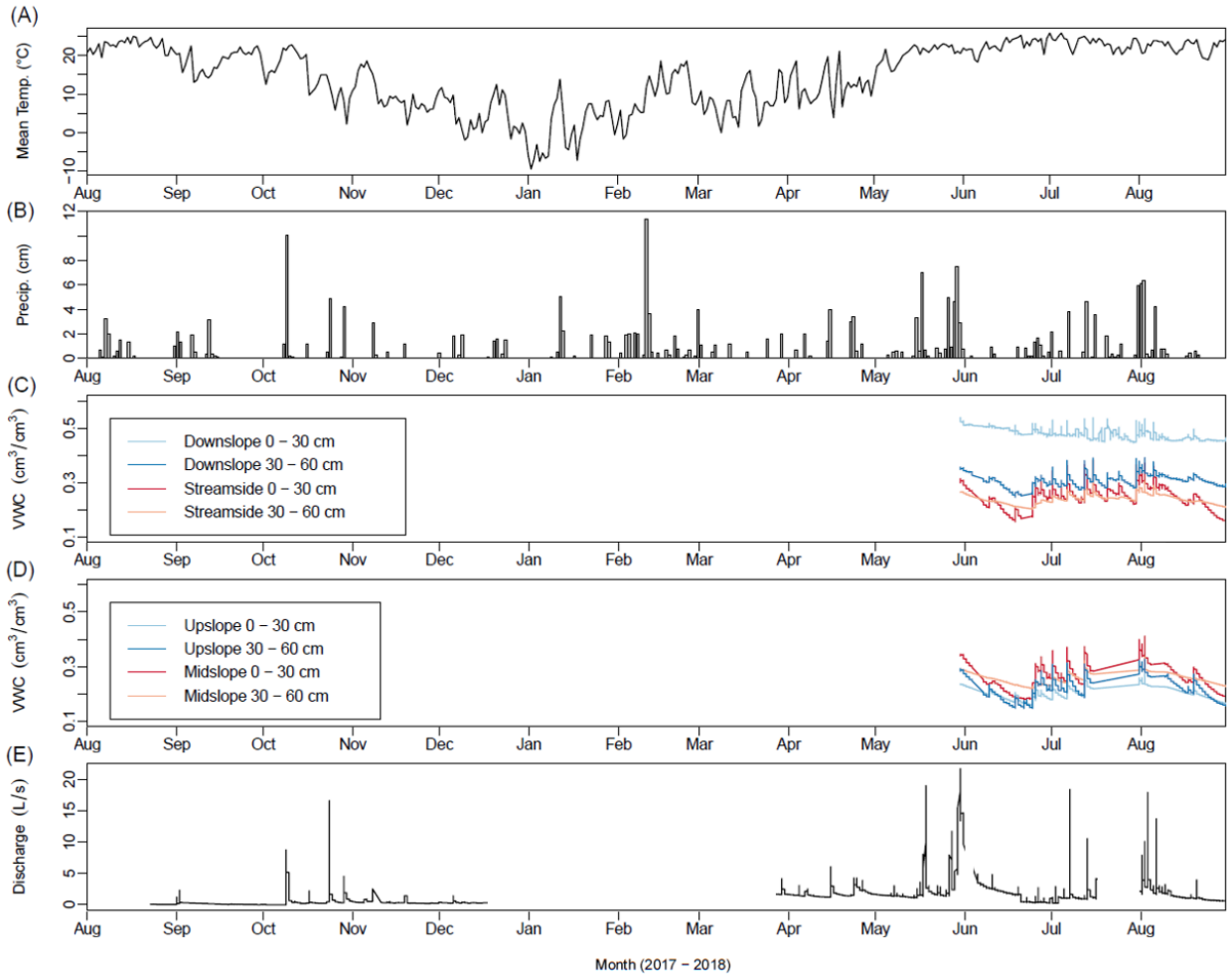

Figure 3.2. Hydroclimate data at Coweeta Hydrologic Laboratory in August 2017 – August 2018. (A) Mean daily temperature (° C) at Climate Station 01 (CS01, latitude 35.07382, longitude -83.47845) (Miniat et al., 2015). (B) Mean daily precipitation (cm) at CS01 (Miniat et al., 2015). (C) Volumetric water content of soil (cm^3 cm^{-3}) at 0 – 30 cm and 30 – 60 cm a streamside and downslope location at the study site. (D) Volumetric water content of soil (cm^3 cm^{-3}) at 0 – 30 cm and 30 – 60 cm a midslope and upslope location at the study site. (E) Streamflow discharge (L s^{-1}) at the flume at the north end of the study site.

Precipitation was high relative to long-term records at Coweeta Hydrologic Laboratory (Figure 3.2b). Total annual precipitation from August 1, 2017 to July 31, 2018 was 1,802 mm, 13% higher than the long-term average (1936 to 2018). While the latter half of 2017 was drier than usual, calendar year 2018 was the wettest year on record; February, May, July, and August 2018 all had precipitation at least 60% higher than the long-term record. May 2018 was an especially wet month with 377 mm of rain, 178% higher than the long-term record.

Soil water content was measured in June – August 2018 and responded to storms throughout the summer (Figure 3.2c and Figure 3.2d). Soil water content was lowest in late June and highest in early August, following several consecutive days of rainfall. Overall mean soil water content was 0.26 cm^3 cm^{-3}. Soil water content was frequently higher in shallow soils than in deeper soils. Mean soil water content in the shallow layer (0 – 30 cm depth) was 0.48, 0.25, 0.26, and 0.20 cm^3 cm^{-3} at the streamside, downslope, midslope, and upslope locations, respectively. Mean soil water content in the deep layer (30 – 60 cm depth) was 0.32, 0.24, 0.25, and 0.22 cm^3 cm^{-3} at the streamside, downslope, midslope, and upslope locations, respectively.

Mean streamflow was 1.2 L s^{-1}, ranging from 0 to 21.7 cm^3 s^{-1} (Figure 3.2e). Streamflow demonstrated flashy behavior in response to storms. Peak flows occurred in summer 2018 after several days of high rainfall. Due to datalogger failure, streamflow data were not collected for approximately four months of the study period.

2. Stable Isotopes of Tree Xylem Water and Environmental Waters

We collected 152 precipitation samples during the study period. We used weekly depth-weighted precipitation $\delta^{18}O$ and $\delta^{2}H$ to generate a local meteoric water line (LMWL), which took the form of $\delta^{2}H = 7.07 \times \delta^{18}O + 8.09$ (Figure 3.3). The slope of the LMWL was slightly less than

that of the global meteoric water line (GMWL), and the intercept was lower than that of the GMWL ($\delta^2H = 8 \times \delta^{18}O + 10$). Precipitation isotope composition ranged from -11.03 $\delta^{18}O$ ‰ and -52.47 δ^2H ‰ in winter to -2.83 $\delta^{18}O$ ‰ and -23.10 δ^2H ‰ in summer.

We analyzed a total of 11 groundwater, 91 stream water, 68 soil water, and 192 tree water samples for stable isotopes of oxygen and hydrogen. Figure 3.3 displays the distribution of water samples in dual isotope space. On average, summer samples had the heaviest isotope composition and least variability, whereas winter samples were isotopically lighter and more variable. Environmental water sources nearly bracketed the observed xylem water compositions. Groundwater experienced the least variability in isotopic composition, ranging from -6.09 to -5.26 ‰ in $\delta^{18}O$ and -35.60 to -29.71 ‰ in δ^2H. Stream water was more variable, ranging from -6.51 to-5.72 ‰ in $\delta^{18}O$ and -37.35 to -30.43 ‰ in δ^2H. Soil water was the most variable environmental water pool, ranging from -8.20 to -3.92 ‰ in $\delta^{18}O$ and -49.28 to -21.60 ‰ in δ^2H. Though groundwater, stream water, and soil water generally fell along the LMWL, tree xylem water experienced variability below the LMWL, showing evidence of evaporation. For precipitation, soil water, and tree water, each season had a significantly different distribution of $\delta^{18}O$ ($p < 0.05$) and δ^2H values ($p < 0.05$). Seasonal differences in $\delta^{18}O$ and δ^2H were not significant for groundwater and stream water.

During the study period, tree water samples typically had lower deuterium excess values than environmental water samples (Figure 3.4). The deuterium excess of stream water and groundwater was confined to the range of 10.98 to 17.11 ‰, while the deuterium excess of tree water ranged from -9.15 to 19.42 ‰. In the drier months (2017), *A. rubrum* had significantly lower deuterium excess than other species. In wetter months (2018), the distribution of deuterium excess

of tree water samples was similar among species. *Q. alba* and *R. maximum* had consistently higher deuterium excess values with smaller distributions, with the exception of *Q. alba* in May 2018.

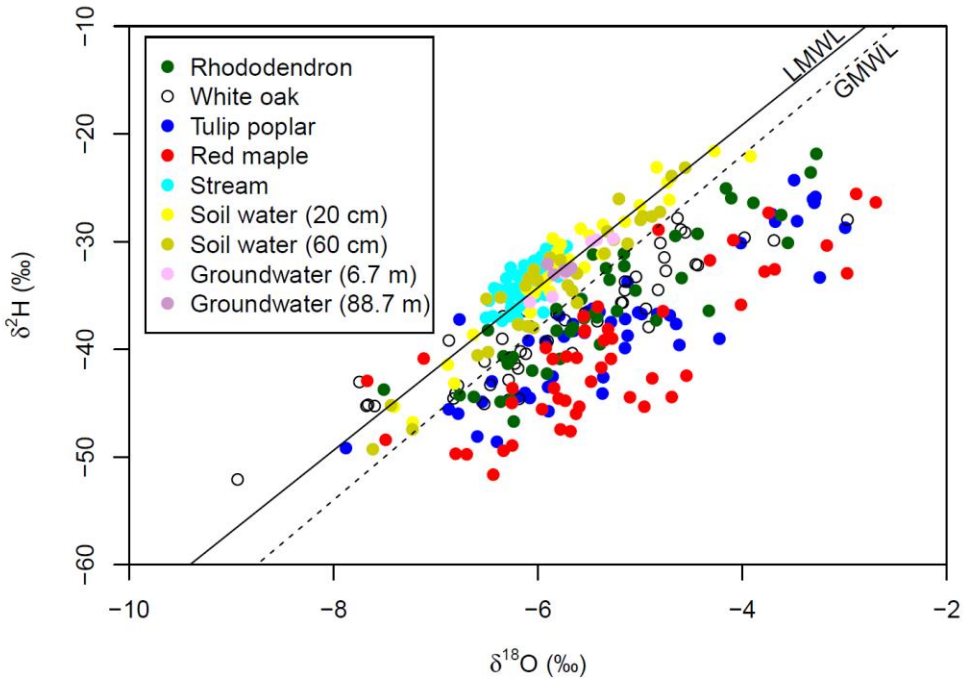

Figure 3.3. Dual isotope plot for tree xylem water, shallow soil water (20 cm depth), deep soil water (60 cm depth), stream water, and groundwater samples for the period of August 2017 – August 2018. The local meteoric water line (LMWL, $\delta^2H = 7.07 \times \delta^{18}O + 8.09$, $R^2 = 0.92$) is shown with a solid line, and global meteoric water line (GMWL, $\delta^2H = 8 \times \delta^{18}O + 10$) is shown with a dashed line.

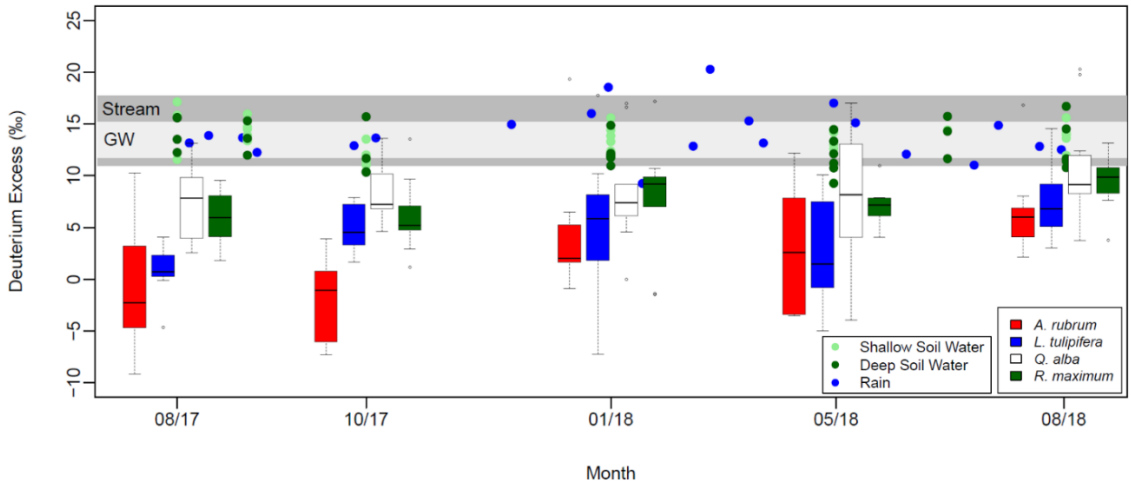

Figure 3.4. Time series of deuterium excess (‰) for all water pools. Stream water and groundwater (GW) had relatively constant deuterium excess and are represented as strips of gray that display their distribution. Rainfall events and lysimeter samples of shallow (20 cm depth) and deep (60 cm depth) soil water are represented as colored points. Distributions of deuterium excess in xylem water are represented by boxplots divided by tree species for each sampling date. Boxplots are not drawn to scale in the x-axis.

3. Seasonal Origins of Tree Xylem Water and Soil Water

The distributions of SOI for each tree species and each soil water depth are displayed in Figure 3.5. Soil water SOI ranged from approximately -2 to 4, and 60% of samples were between 1 and 3, indicating that throughout the year, most soil water originated as summer precipitation. The distribution of soil water SOI varied significantly with depth ($p < 0.05$); soil water at 20 cm depth was more likely to be sourced from summer precipitation than soil water at 60 cm depth. Low SOI values were more prevalent in xylem water than soil water, meaning that trees used more water originating in the winter than in the summer. Tree water SOI ranged from approximately -6 to 3. The distribution of tree water SOI varied significantly by species ($p < 0.001$). Pairwise comparisons reveal that the SOI of *A. rubrum* was significantly lower than *Q. alba* and *R. maximum* ($p < 0.001$) and that *L. tulipifera* was significantly lower than *R. maximum* ($p < 0.001$). Distributions of SOI did not differ significantly between *Q. alba* and *R. maximum*.

The distribution of SOI among tree species through time is shown in Figure 3.6. The overall SOI of tree water varied over time, and the pattern of SOI over time varied by species. SOI for all tree species was highest on the first sampling date of August 2017, sharply dropping in October 2017 and slowly increasing through time until August 2018. *A. rubrum* trees used water with the lowest SOI for the first three sampling dates, but *L. tulipifera* used water with lower SOI than *A. rubrum* for the final two sampling dates. The SOI of *R. maximum* followed the season of the sampling date; *R. maximum* had higher SOI during summer sampling dates and lower SOI during fall and winter sampling dates. *Q. alba* experienced the least variability in SOI during the study period. *L. tulpifera* appeared to use more well-mixed water throughout the year, neither relying on one type of precipitation (strongly winter or summer) nor recent precipitation. There was more overlap in distribution of SOI between species during the transitional months, October and May.

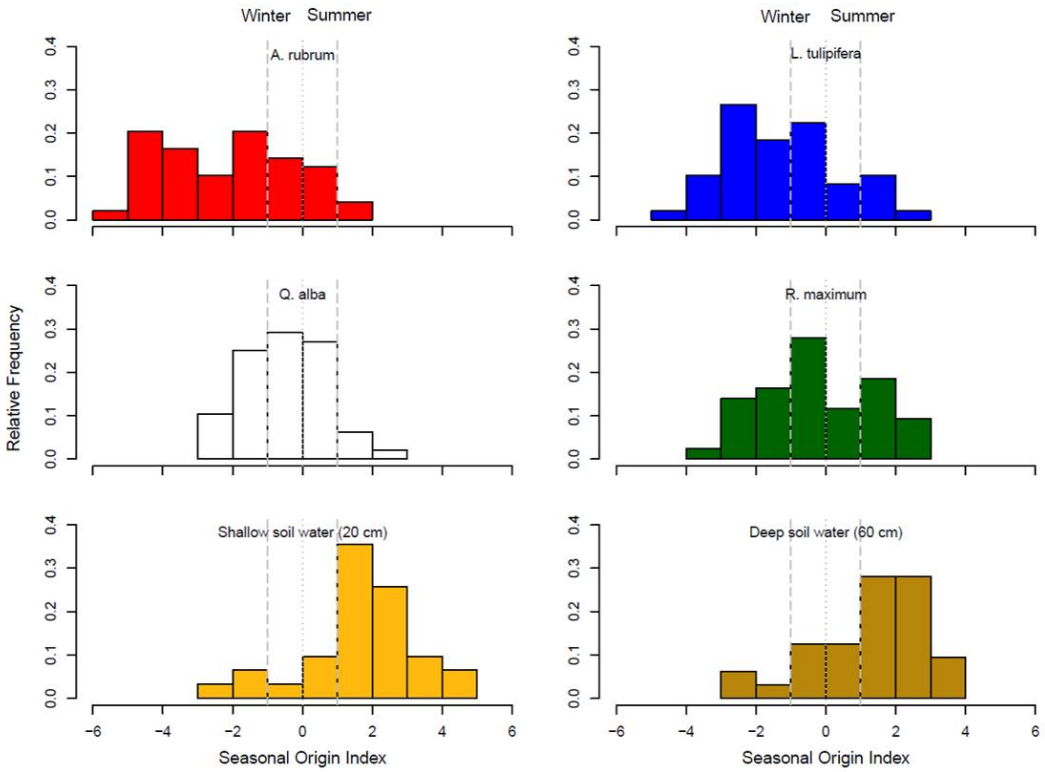

Figure 3.5. Distributions of the seasonal origin index in xylem water of *A. rubrum*, *L. tulipifera*, *Q. alba*, and *R. maximum* and soil water (20 cm and 60 cm depths) at the study site.

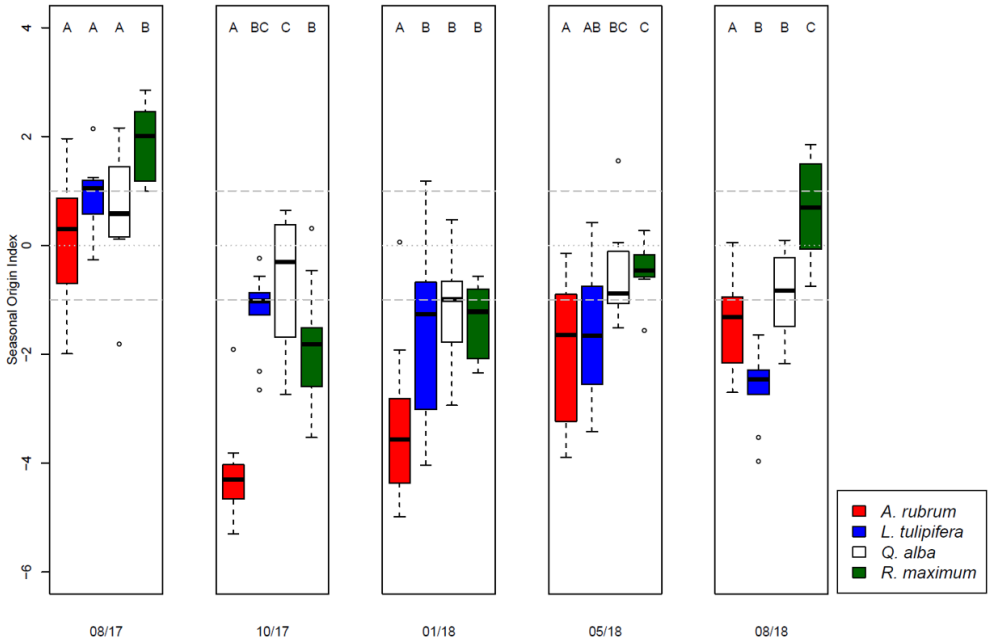

Figure 3.6. Time series of the distributions of seasonal origin index in xylem water of *A. rubrum*, *L. tulipifera*, *Q. alba*, and *R. maximum*. Samples are marked as outliers (shown as circles) if their value is outside 1.5 times the interquartile range above the upper quartile or below the lower quartile. Letters indicate significant differences in sample distributions by Kruskal-Wallis tests.

4. Water Age

The fractions of young water (i.e., water less than 2.3 ± 0.8 months old) in water samples are reported in Table 3.2. Young water made up about 5% of all groundwater samples, 9% for shallow groundwater (depth 6.7 m) and 2% for deep groundwater (depth 88.7 m). Young water made up about 5% of soil water, 10% for shallow soil water (60 cm) and 1% for deep soil water (depth 60 cm). Tree water was younger than environmental waters. Young water made up about 11% of tree xylem water. Streamside trees had more young water (12%) than upslope trees (5%), but midslope trees had more young water (17%) than streamside trees.

Tree species significantly influenced the distribution of young water fraction ($p < 0.05$). *R. maximum* had the youngest water (18%), followed by *A. rubrum* (15%), *L. tulipifera* (8%), and *Q. alba* (6%). The distribution of young water in *R. maximum* was only statistically significantly greater than *L. tulipifera* ($p < 0.05$). Only *L. tulipifera* had samples with young water fractions that overlapped the young water fraction of environmental waters. However, there was no linear relationship between young water fraction and hillslope gradient of trees ($R^2 = 0.01$).

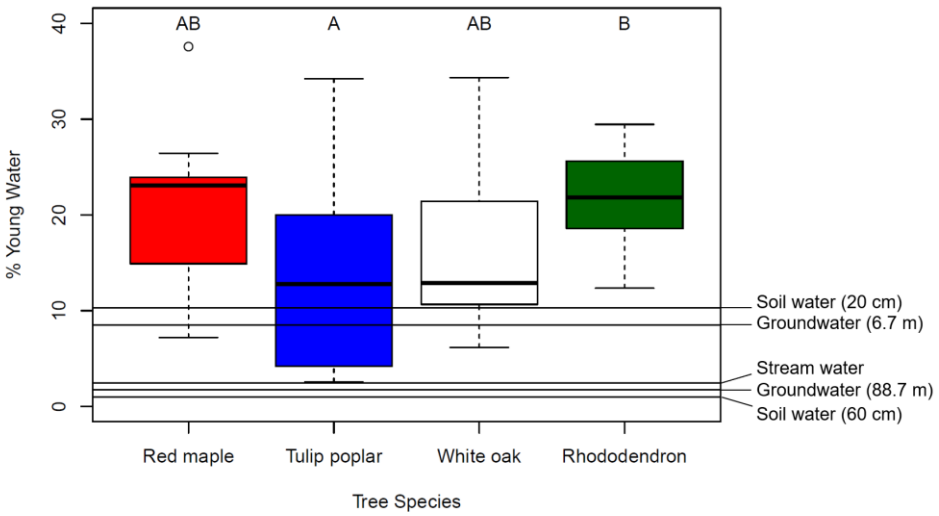

Figure 3.7. Distributions of the percentage of young water by tree species. Samples are marked as outliers (shown as circles) if their value is outside 1.5 times the interquartile range above the upper quartile or below the lower quartile. The age of soil water, groundwater, and stream water pools is represented by lines. Letters indicate significant differences in sample distributions by Kruskal-Wallis tests.

Table 3.2. Mean percentage of young water in groups of water samples, where young water is defined as water that entered the soil as precipitation within the last 2.3 ± 0.8 months (Kirchner, 2016).

Water Pool	Cosine Coefficient	Sine Coefficient	Amplitude (‰)	% Young Water
Groundwater	0.22	-0.05	0.22	4.94
Shallow groundwater (6.7 m)	0.36	-0.10	0.38	8.48
Deep groundwater (88.7 m)	0.07	0.03	0.08	1.76
Stream water	0.03	-0.10	0.11	2.45
Soil water	-0.04	0.21	0.22	4.83
Shallow soil water (20 cm)	-0.08	0.45	0.46	10.29
Deep soil water (60 cm)	-0.04	-0.02	0.04	0.97
Trees	-0.50	0.05	0.50	11.29
Streamside trees	-0.49	0.18	0.52	11.76
Midslope trees	-0.75	0.01	0.75	16.76
Upslope trees	-0.22	-0.03	0.22	4.99
R. maximum trees	-0.79	-0.03	0.79	17.61
Streamside *R. maximum* trees	-0.75	0.09	0.75	16.86
Midslope *R. maximum* trees	-0.91	-0.03	0.91	20.33
Upslope *R. maximum* trees	-0.74	-0.14	0.75	16.88
A. rubrum trees	-0.68	-0.10	0.69	15.41
Streamside *A. rubrum* trees	-0.69	0.07	0.69	15.50
Midslope *A. rubrum* trees	-1.01	0.08	1.01	22.72
Upslope *A. rubrum* trees	-0.18	-0.49	0.52	11.67
L. tulipifera trees	-0.37	0.08	0.38	8.41
Streamside *L. tulipifera* trees	-0.43	0.11	0.44	9.87
Midslope *L. tulipifera* trees	-0.48	-0.01	0.48	10.83
Upslope *L. tulipifera* trees	-0.15	0.19	0.24	5.40
Q. alba trees	-0.21	0.20	0.29	6.48
Streamside *Q. alba* trees	-0.16	0.51	0.53	11.93
Midslope *Q. alba* trees	-0.59	-0.02	0.59	13.21
Upslope *Q. alba* trees	0.02	0.24	0.24	5.36

Discussion

1. Stable Isotope Composition

The isotope ratios of environmental waters (groundwater, stream water, and soil water) were within the range of the LMWL, showing little evidence of evaporation (Figure 3.3). The isotope composition of groundwater and stream water were very similar, especially for deep groundwater, suggesting that streams are driven by deep, well-mixed baseflow. Although soil water had differences in SOI and young water fractions between the shallow and deep layers, they exhibit similar ranges in isotope composition. Though both soil layers contained water at each end of the isotopic spectrum at some point during the study period, the timing of the isotope

composition led to differences in interpretation of water age. Tree water isotopes were evaporated compared to environmental waters, a finding consistent with past studies (Brooks et al., 2010; Bowling et al., 2016; Evaristo et al., 2015; Jia et al., 2017). Tree water isotope composition was not wholly contained within the range of environmental waters, which we attribute to the fact that lysimeters fail to collect bulk soil water (Sprenger, 2018).

Deuterium excess in tree water was much lower than in environmental waters, likely due to evaporation between soil infiltration and root uptake (Figure 3.4). The especially low deuterium excess values in *A. rubrum* and *L. tulipifera* mean that these trees source water from shallow, evaporated soil waters, which may include water that is not sampled by lysimeters because it is very shallow (less than approximately 20 cm depth) or tightly bound (greater than -0.06 MPa tension). Indeed, many trees have high fine root density in the shallow soil layer (Bréda et al., 1995). In contrast, *Q. alba* and *R. maximum*, which had higher deuterium excess values, likely uptake water from less evaporated water sources. The range of deuterium excess in *Q. alba* frequently overlapped the range of ground and stream water, further suggesting that this tree species uses deep soil water that is similar to groundwater. Matheny et al. (2016) also found that deuterium excess in *A. rubrum* was lower than another oak species, *Q. rubra* throughout summer months. Studies have shown that rooting depth can be inferred from deuterium excess, with lower deuterium excess values implying shallower rooting depth (Dawson, 1993; West et al., 2012). This relationship is consistent with known rooting depths for the deciduous trees: *Q.* spp in the southeast have roots as deep as 430 cm (Biswell, 1935; Weaver & Kramer, 1932), *L. tulipifera* has roots as deep as 120 cm (Francis, 1979), and *A. rubrum* has roots as deep as 110 cm (Haag et al., 1989).

Several studies (Bush et al., 1992; Dawson and Ehleringer, 1991; Thorburn and Walker, 1993) demonstrated that mature, riparian trees in a variety of ecosystems use groundwater, not

stream water, to support transpiration. Bowling et al. (2016) also found that streamside trees do not use stream water but were unable to identify groundwater as the tree water source. Our findings are similar to Dawson and Ehleringer (1991) in that *Q. alba* appears to uptake groundwater. However, our results also agree with Bowling et al. (2016) because the isotope composition of *A. rubrum*, *L. tulipifera*, and *R. maximum* does not reflect environmental waters. Generally, we can conclude that streamside trees at our study site do not use stream water directly.

2. Seasonal Origins of Tree Xylem Water and Soil Water

According to the SOI, the majority of shallow soil water samples (70%) originated predominantly from summer precipitation, 10% originated predominantly from winter precipitation, and 20% represented a mixture of precipitation from all seasons. In deep layers, the pattern was different. Only 20% of soil water samples originated predominantly from summer precipitation, 30% originated predominantly from winter precipitation, and half of soil water samples were a mixture of precipitation from all seasons. The distribution of SOI for shallow and deep soil water was strikingly similar to those found in Switzerland by Allen et al. (2019), though we found a larger range in values due to sampling in seasons beyond summer. We can use this understanding of soil water to explain seasonal tree water dynamics.

A. rubrum had the lowest SOI values of all samples, suggesting that its xylem water originated primarily from winter precipitation; 70% of samples indicated winter origin, and 26% of samples indicated mixed origin. *L. tulipifera* displayed a similar distribution of SOI, though not as extreme as *A. rubrum*. In contrast, *R. maximum* had the highest SOI values for tree water, with xylem water samples split evenly among winter-origin precipitation, summer-origin precipitation, and mixed origins. *Q. alba* primarily used water from seasonally mixed origins. Similar to Allen

et al. (2019), SOI values were noticeably lower in tree xylem water than in soil water. Allen et al. (2019) determined that in the summer, xylem water from the oak species *Q. rubur* L. showed a predominance of winter precipitation. Our oak species showed a predominance of winter precipitation in summer 2018 but a predominance of mixed precipitation in summer 2017. Because the ratio of winter-to-summer precipitation was greater in 2018 than 2017, we conclude that oak trees are using deeper water, regardless of its seasonal source. SOI appears to be highly dependent on recent precipitation, so it should be investigated over multiple years to realistically represent tree water source.

We can relate seasonal difference sin SOI values to the plumbing of woody stems. *A. rubrum*, *L. tulipifera*, and *R. maximum* have diffuse-porous xylem anatomy, and *Q. alba* has ring-porous xylem anatomy. Diffuse-porous wood has narrow vessels that are evenly dispersed across the growth ring and retain function year-round, leading to more functional sapwood area and greater water use. Diffuse-porous trees limit transpiration by stomatal closure as soil becomes drier or atmospheric vapor pressure deficit increases (Wheeler & Baas, 1993). In contrast, ring-porous wood has large conduits that embolize in freeze-thaw events and under very dry conditions, so it has less functional sapwood area and lower water use. Thus, ring-porous trees prefer a physiologically riskier approach that maintains high photosynthetic uptake despite low soil moisture (Zimmermann, 1983). Figure 3.6 shows that *Q. alba* uses a relatively consistent source of water year-round, as its ring-porous xylem maintains similar water use across a variety of environmental conditions. The seasonal source of *A. rubrum* and *L. tulipifera* water varies greatly during the year, perhaps indicating changes in transpiration control. These diffuse-porous species may also pull water from a greater variety of water sources to maintain their higher rate of water uptake. *R. maximum* did not behave similarly to the other diffuse-porous species, likely because it

is a small, evergreen shrub. Instead, the water source of *R. maximum* followed seasonal variations, indicating that it is likely shallow-rooted and uses recent precipitation for transpiration.

3. Soil and Tree Water Age

Calculations of young water fraction reveal that groundwater contains about 5% young water, stream water contains about 2% young water, shallow soil water contains about 10% young water, and deep soil water contains about 1% young water (Table 3.2). Tree water samples had greater young water fractions than environmental waters, containing about 11% young water. The young water fractions of each tree species corroborate the SOI results and provide insight into specific water ages, unlike the coarse scale of the SOI. *R. maximum* xylem water samples had the largest fraction of young water and smallest distribution of young water fraction (Figure 3.7). *A. rubrum* had the second largest young water fraction and a slightly wider distribution of young water fraction. *L. tulipifera* had a smaller young water fraction and a large distribution of young water fraction that overlapped environmental waters. *Q. alba* had the smallest young water fraction. These findings have implications for drought vulnerability. Tree species that rely primarily on young water, such as *R. maximum* and *A. rubrum*, may be more vulnerable during periods of drought. Trees that rely on older water or use water from a variety of ages, such as *Q. alba* and *L. tulipifera*, may experience less water stress during droughts.

Jasechko et al. (2016) reported that the fraction of young streamflow is expected to decrease with increasing topographic gradient. Similarly, we found that upslope trees along our hillslope gradient had older water. However, the relationship was not significant across the full range of hillslope gradients, because midslope trees had more young water than streamside (downslope) trees. One interpretation is that soil water mixes with much older groundwater in

riparian areas, which are topographically convergent zones and also zones of groundwater discharge. Thus, streamside trees could have access to relatively old groundwater. Another reasoning is that the topographic gradient in this study site was not as large as observed in Jasechko et al. (2016), so we may not expect to observe similar patterns.

The environmental waters and tree waters in this study were older than expected for this study site compared to young water fractions reported in Chapter 1 and other literature (e.g., Jasechko et al., 2016; Song et al., 2016). The results of the young water fraction analysis may be difficult to interpret in this case because the isotope composition of precipitation at Coweeta does not exhibit strong sinusoidal behavior.

4. Limitations and future work

This study aimed to characterize typical tree water source and residence time in the southern Appalachians. However, precipitation at Coweeta Hydrologic Laboratory was unique in 2018—it was the wettest year on record. Furthermore, precipitation was low in fall 2017. Given the unusual precipitation quantities during the study period, it may be difficult to generalize our results to typical years. Moreover, the isotope composition of precipitation did not exhibit strong sinusoidal behavior during the study period. The southern Appalachian region of North Carolina in particular has little variability between water pools (Evaristo, 2015). The SOI and young water fraction rely on strong seasonal variations in isotope composition and substantial differences between water pools, so new methods may be needed for regions with low seasonal variability. Beyond these site-based limitations, several methodological improvements could have been made to the study. Lysimeters collect mobile water that is known to reflect infiltrating precipitation, excluding bulk water that exhibits an evaporation signal (Brooks et al., 2010). By excluding bulk

water from our analysis, we cannot fully contain the range of isotope ratios within tree xylem water by soil water isotope composition. Although groundwater samples were collected, the wells were located about 200 m from the study site, and depth to groundwater level was not recorded.

Because the Picarro Induction Module is not a widely-used method for the analysis of tree core isotopes, our results should be validated by analyzing tree cores by cryogenic extraction and isotope-ratio mass spectrometry (Lazarus et al., 2016). Future work should also extend this study to drought conditions. Some tree species, especially ring-porous trees such as *Q. alba*, embolize during extremely dry periods and may have different water use behavior during drought.

Conclusion

To characterize tree water use in the southern Appalachians, we collected seasonal samples of soil water, stream water, groundwater, precipitation, and tree xylem for one year and analyzed their stable isotope composition ($\delta^{18}O$ and $\delta^{2}H$). We examined four tree species that represent two xylem anatomies, R*hododendron maximum* (rhododendron), *Acer rubrum* (red maple), *Liriodendron tulipifera* (tulip poplar), and *Quercus alba* (white oak). We analyzed the isotope composition, seasonal origin, and age of these samples. We found that precipitation, soil water, and tree water, but not groundwater or stream water, had significantly different isotope compositions in each season. Soil water that was collected from lysimeters had the most isotopic variability among the environmental water pools, but it did not fully bracket the range of variability observed in tree water. Deuterium excess of tree water was consistently lower than environmental waters. In dry months, *A. rubrum* had significantly lower deuterium excess than other species, while in wet months, deuterium excess was similar among species. We found that streamside trees do not use stream water as a source of transpiration.

The seasonal origin of soil water was significantly influenced by depth, as shallow soil water was sourced more from summer precipitation than deeper soils, which represented a mix of multiple seasons. Generally, tree water was primarily sourced from winter precipitation or mixed sources and was significantly influenced by species. *A. rubrum* and *L. tulipifera* used more winter precipitation, *Q. alba* used mixed precipitation, and *R. maximum* used water from winter, summer, or mixed sources. *R. maxmimum* water was the youngest of all tree species, followed by *A. rubrum*, *L. tulipifera*, and *Q. alba*. These findings follow the expected behavior of these trees with respect to xylem anatomy; diffuse-porous species used a larger quantity of water from a variety of sources, while ring-porous species used older water from a single source. There was no apparent relation between soil or tree water age and topographic gradient.

Our findings have implications for the vulnerability of forests to drought, as certain species prefer to use young water that entered the watershed as precipitation within the last several months. This work advances our understanding of ecohydrological separation in humid, forested catchments with relatively high frequency sampling of soil and xylem water, which may aid in the development of mechanistic models of ecohydrological interaction.

REFERENCES

Allen, M.R. & Ingram, W.J. (2002). Constraints on future changes in climate and the hydrologic cycle. *Nature 419*: 224-232. doi: 10.1038/nature01092.

Allen, S. T., Kirchner, J. W., Braun, S., Siegwolf, R. T., & Goldsmith, G. R. (2019). Seasonal origins of soil water used by trees. *Hydrology and Earth System Sciences Discussions*. doi:10.5194/hess-2018-554.

Barbeta, A., Jones, S.P., Clavé, L., Wingate, L., Gimeno, T.E., Fréjaville, B., et al. (in review). Hydrogen isotope fractionation affects the identification and quantification of tree water sources in a riparian forest. *Hydrology and Earth System Sciences*. doi: 10.5194/hess-2018-402.

Berry, Z.C., Evaristo, J., Moore, G., Poca, M., Steppe, K., Verrot, L., et al. (2016). The two water worlds hypothesis: Addressing multiple workinghypotheses and proposing a way forward. *Ecohydrology 11*(3). doi: 10.1002/eco.1843.

Biswell, H.H. (1935). Effects of environment upon the root habits of certain deciduous forest trees. *Botanical Gazette 96*(4): 676-708. doi: 10.1086/334517.

Bréda, N., Grainer, A., Barataud, F., & Moyne, C. (1995). Soil water dynamics in an oak stand. *Plant and Soil 172*(1): 17-27. doi: 10.1007/BF00020856.

Bosch, J.M., & Hewlett J.D. (1982). A review of catchment experiments to determine the effect of vegetation changes on water yield and evapotranspiration. *Journal of Hydrology 55*(1-4): 3-23. doi: 10.1016/0022-1694(82)90117-2.

Bowling, D.R., Schulze, E.S., & Hall, S.J. (2016). Revisiting streamside trees that do not use stream water: can the two water worlds hypothesis and snowpack isotopic effects explain a missing water source? *Ecohydrology 10*(1). doi: 10.1002/eco.1771.

Brantley, S., Ford, C.R., & Vose, J.M. (2013). Future species composition will affect forest water use after loss of eastern hemlock from southern Appalachian forests. *Ecological Applications 23*(3): 777-790. doi: 10.1890/12-0616.1.

Brooks, J. R., Barnard, H. R., Coulombe, R., & McDonnell, J. J. (2010). Ecohydrologic separation of water between trees and streams in a Mediterranean climate. *Nature Geoscience*, *3*(2), 100–104. doi:10.1038/NGEO722.

Brown, T.C., Hobbins, M.T., & Ramirez, J.A. (2008). Spatial distribution of water supply in the coterminous United States. *Journal of the American Water Resources Association 44*(6): 1474-1487. doi: 10.1111⁄j.1752-1688.2008.00252.x.

Busch, D.E., Ingraham, N.L, & Smith, S.D. (1992). Water Uptake in Woody Riparian Phreatophytes of the Southwestern United States: A Stable Isotope Study. *Ecological Applications 2*(4): 450-459. doi: 10.2307/1941880.

Cernusak, L.A., Barbour, M.M., Arndt, S.K., Cheesman, A.W., English, N.B., Field, T.S., et al. (2016). Stable isotopes in leaf water of terrestrial plants. *Plant, Cell & Environment 39*(5): 1087-1102. doi: 10.1111/pce.12703.

Dawson, T.D. (1993). Hydraulic lift and water use by plants: implications for water balance, performance and plant-plant interactions. *Oecologia 95*(4): 565-574. doi: 10.1007/BF00317442.

Dawson, T.D., & Ehleringer, J.R. (1991). Streamside trees that do not use stream water. *Nature 350*(6316): 335-337. doi: 10.1038/350335a0.

Day Jr., F.P., Phillips, D.L., & Monk, C.D. (1988). Forest Communities and Patterns. In *Forest hydrology and ecology at Coweeta* (pp. 141–149). New York: Springer-Verlag.

Emanuel, R. E. (2018). Climate Change in the Lumbee River Watershed and Potential Impacts on the Lumbee Tribe of North Carolina. *Journal of Contemporary Water Research & Education, 163*(1), 79-93. doi: 10.1111/j.1936-704X.2018.03271.x.

Evaristo, J., Jasechko, S., & McDonnell, J.J. (2015). Global separation of plant transpiration from groundwater and streamflow. *Nature 525*: 91-94. doi: 10.1038/nature14983.

Evaristo, J., McDonnell, J.J., & Scholl, M.A., Bruijnzeel, L.A., Chun, K.P. (2016). Insights into plant water uptake from xylem-water isotope measurements in two tropical catchments with contrasting moisture conditions. *Hydrological Processes 30*(18). doi: 10.1002/hyp.10841.

Ford, C.R., Hubbard, R.M., & Vose, J.M. (2011a). Quantifying structural and physiological controls on variation in canopy transpiration among planted pine and hardwood species in the southern Appalachians. *Ecohydrology 4*(2): 183-195. doi: 10.1002/eco.136.

Ford, C.R., Laseter, S.H., Swank, W.T., & Vose, J.M. (2011b). Can forest management be used to sustain water-based ecosystem services in the face of climate change? *Ecological Applications 21*(6): 2049-2067. doi: 10.1890/10-2246.1.

Francis, J.K. (1979). Yellow-Poplar Rooting Habits. Research Note SO-246. Department of Agriculture, Forest Service, Southern Forest Experiment Station. https://www.srs.fs.usda.gov/pubs/rn/rn_so246.pdf.

Geris, J., Tetzlaff, D., McDonnell, J.J., Soulsby, C. (2015). The relative role of soil type and tree cover on water storage and transmission in northern headwater catchments. *Hydrological Processes 29*(7): 1844-1860. doi: 10.1002/hyp.10289.

Goldsmith, G.R., Munoz-Villers, L.E., Holwerda, F., McDonnell, J.J., Asbjornsen, H., & Dawson, T.D. (2012). Stable isotopes reveal linkages among ecohydrological processes in a seasonally dry tropical montane cloud forest. *Ecohydrology 5*(6): 779-790. doi: 10.1002/eco.268.

Hagg, C.L., Johnson, J.E., & Erdmann, G.G. (1989). Rooting depths of red maple (*Acer Rubrum* L.) on various sites in the lake states. Research Note NC-347. United States Department of Agriculture, Forest Service, North Central Forest Experimental Station. https://www.ncrs.fs.fed.us/pubs/rn/rn_nc347.pdf.

Hervé-Fernandez, P., Oyarzún, C.E., & Woelfl, S. (2016). Throughfall enrichment and stream nutrient chemistry in small headwater catchments with different land cover in southern Chile. *Hydrological Processes 30*(26): 4944-4955. doi: 10.1002/hyp.11001.

Iverson, L., Prasad, A., & Matthews, S. (2008). Modeling potential climate change impacts on the trees of the northeastern United States. *Mitigation and Adaptation Strategies for Global Change 13*(5-6): 487-516. doi: 10.1007/s11027-007-9129-y.

Jasechko, S., Kirchner, J. W., Welker, J. M., & McDonnell, J. J. (2016). Substantial proportion of global streamflow less than three months old. *Nature Geoscience*, *9*(2), 126–129. doi:10.1038/ngeo2636.

Jia, G., Lui, Z., Chen, L., & Yu, X. (2017). Distinguish water utilization strategies of trees growing on earth-rocky mountainous area with transpiration and water isotopes. *Ecology and Evolution 7*(24): 10640-10651. doi: 10.1002/ece3.3584.

Jones, J.A. (2000). Hydrologic processes and peak discharge response to forest removal, regrowth, and roads in 10 small experimental basins, western Cascades, Oregon. *Water Resources Research 36*(9): 2621-2642. doi: 10.1029/2000WR900105.

Jones, J.A., & Grant, G.E. (1996). Peak flow responses to clear-cutting and roads in small and large basins, western Cascades, Oregon. *Water Resources Research 32*(4): 959-974. doi: 10.1029/95WR03493.

Kendall, C., & McDonnell, J. J. (1998). Isotope Tracers in Catchment Hydrology. Amsterdam: Elsevier Science.

Kim, Y., Band, L.E., & Song, C. (2014). The influence of forest regrowth on the stream discharge in the North Carolina piedmont watersheds. *Journal of the American Water Resources Association 50*(1): 57-73. doi: 10.1111/jawr.12115.

Kirchner, J. W. (2016). Aggregation in environmental systems – Part 1: Seasonal tracer cycles quantify young water fractions, but not mean transit times, in spatially heterogeneous catchments. *Hydrology and Earth System Sciences*, *20*(1), 279–297. doi:10.5194/hess-20-279-2016.

Knox, J.C. (2000). Sensitivity of modern and Holocene floods to climate change. *Quaternary Science Reviews 19*(1-5): 439-457. doi: 10.1016/S0277-3791(99)00074-8.

Lazarus, B.E., Germino, M.J., Vander Veen, J.L. (2016). Online induction heating for determination of isotope composition of woody stem water with laser spectrometry: a methods assessment. *Isotopes in Environmental and Health Studies 52*(3): 309-325. doi: 10.1080/10256016.2016.1141205.

Luce, C.H., & Holden, Z.A. (2009). Declining annual streamflow distributions in the Pacific Northwest United States, 1948-2006. *Geophysical Research Letters 36*(16). doi: 10.1029/2009GL039407.

Matheny, A.M., Fioella, R.P., Bohrer, G., Poulsen, C.J., Morin, T.H., Wunderlich, A., et al. (2016). Contrasting strategies of hydraulic control in two codominant temperate tree species. *Ecohydrology 10*(3). doi: 10.1002/eco.1815.

Michelsen, N., van Geldern, R., Roßmanna, Y., Bauera, I., Schulz, S., & Barth, J.A.C., et al. (2018). Comparison of precipitation collectors used in isotope hydrology. *Chemical Geology, 488*, 171–179. doi: 10.1016/j.chemgeo.2018.04.032.

Milly, P.C.D., Betancourt, J., Falkenmark, M., Hirsch, R., Kundzewicz, W., Lettenmaier, D.P., et al. (2008). Stationarity is dead: Whither water management? *Science 319*(5863): 573-574. doi: 10.1126/science.1151915.

Miniat, C.F., Laseter, S.H., Swank, W.T., & Swift Jr., L.W. (2015). Daily air temperature, relative humidity, vapor pressure, PPFD, wind speed and direction for climate stations at the Coweeta Hydrologic Lab, North Carolina. *Forest Service Research Data Archive*. doi:10.2737/RDS-2015-0042.

Miniat, C.F., Laseter, S.H., Swank, W.T., & Swift Jr., L.W. (2017). Daily precipitation data from recording rain gages (RRG) at Coweeta Hydrologic Lab, North Carolina. *Forest Service Research Data Archive*. doi:10.2737/RDS-2017-0031.

National Cooperative Soil Survey (2004). Saunook Series. *Official Soil Series Descriptions*. https://soilseries.sc.egov.usda.gov/OSD_Docs/S/SAUNOOK.html.

Nippgen, F., McGlynn, B.L, Emanuel, R.E., & Vose, J.M. (2016). Watershed memory at the Coweeta Hydrologic Laboratory: The effect of past precipitation and storage on hydrologic response. *Water Resources Research 52*(3), 1673-1695. doi: 10.1002/2015WR018196.

Postel, S.L. (2000). Entering an era of water Scarcity: the challenges ahead. *Ecological Applications 10*(4): 941-948. doi: 10.1890/1051-0761(2000)010[0941:EAEOWS]2.0.CO;2.

R Core Team (2018). R: A language and environment for statistical computing. R Foundation for Statistical Computing, Vienna, Austria. http://www.R-project.org/.

Rice, J. S., Emanuel, R. E., Vose, J. M., & Nelson, S. A. (2015). Continental US streamflow trends from 1940 to 2009 and their relationships with watershed spatial characteristics. *Water Resources Research, 51*(8), 6262-6275. doi: 10.1002/2014WR016367.

Seager, R., Ting, M., Held, I., Kushnir, Y., Lu, J., Vecchi, G., et al. (2008). Model Projections of an Imminent Transition to a More Arid Climate in Southwestern North America. *Science 316*(5828): 1181-1184. doi: 10.1126/science.1139601.

Seager, R., Tzanova, A., Nakamura, J. (2009). Drought in the Southeastern United States: Causes, Variability over the Last Millennium, and the Potential for Future Hydroclimate Change. *Journal of Climate 22*(19): 5021-5045. doi: 10.1175/2009JCLI2683.1.

Singh, N.K., Emanuel, R.E., & McGlynn, B.L. (2016). Variability in isotopic composition of base flow in two headwater streams of the southern Appalachians. *Water Resources Research 52*(6), 4264-4279. doi: 10.1002/2015WR018463.

Singh, N.K., Emanuel, R.E., Nippgen, F., McGlynn, B.L., & Miniat, C.F. (2018). The Relative Influence of Storm and Landscape Characteristics on Shallow Groundwater Responses in Forested Headwater Catchments. *Water Resources Research 54*(12), 9883-9900. doi: 10.1029/2018WR022681.

Soil Survey Staff, Natural Resources Conservation Service, United States Department of Agriculture. (2018, September 11). Web Soil Survey. Retrieved from https://websoilsurvey.sc.egov.usda.gov.

Song, C., Wang, G., Liu, G., Mao, T., Sung, X., Chen, X. (2016). Stable isotope variations of precipitation and streamflow reveal the young water fraction of a permafrost watershed: *Hydrological Processes, 31*(4), 935-947. doi: 10.1002/hyp.11077.

Sprenger, M., Tetzlaff, D., Buttle, J., Laudon, H., Leistert, H., Mitchell, C.P.J., et al. (2018). Measuring and modeling stable isotopes of mobile and bulk soil water. *Vadose Zone Journal 17*(1). doi: 10.2136/vzj2017.08.0149.

Sprenger, M., Tetzlaff, D., Buttle, J., Laudon, H., & Soulsby, C. (2018). Water ages in the critical zone of long-term experimental sites in northern latitudes. *Hydrology and Earth System Sciences, 22*, 3965–3981. doi:10.5194/hess-22-3965-2018.

Swank, W. T., & Crossley, Jr., D. A. (1988). Introduction and Site Description. In *Forest hydrology and ecology at Coweeta* (pp. 3–16). New York: Springer-Verlag.

Swank, W. T. & J. E. Douglass. (1975). Nutrient flux in undisturbed and manipulated forest ecosystems in the southern Appalachian Mountains., in *Proceedings of the Tokyo Symposium in the Hydrological Characteristics of River Basins,* Int. Assoc. of Hydrol. Sci., Washington, D.C.

Swift Jr., L.W, Cunningham, G.B., & Douglass, J.E. (1988). Climatology and Hydrology. In *Forest hydrology and ecology at Coweeta* (pp. 35–56). New York: Springer-Verlag.

Tanweer, A., Groning, M., Van Duren, M., Jaklitsch, M., & Poltenstein, L. (2009). Stable isotope internal laboratory water standards: Preparation, calibration, and storage, International Atomic Energy Agency technical procedure note 43.

Thorburn, P. J., & Walker, G. R. (1993). The Source of Water Transpired by Eucalyptus camaldulensis: Soil, Groundwater, or Streams? In J. Ehleringer, A. Hall, & G. Farquhar (Eds.), *Stable Isotopes and Plant Carbon-water Relations* (pp. 511–527). San Diego: Academic Press, Inc.

Weaver, J.E., & Kramer, J. (1932). Root system of *Quercus macrocarpa* in relation to the invasion of prairie. *Botanical Gazette 94*(1): 51-85. doi: 10.1086/334284.

West, A.G., Dawson, T.E., February, E.C., Midgley, G.F., Bond, W.J, & Aston, T.L. (2012). Diverse functional responses to drought in a Mediterranean-type shrubland in South Africa. *New Phytologist 195*(2): 396-407. doi: 10.1111/j.1469-8137.2012.04170.x.

Wheeler, E.A. & Baas, P. (1993). The potentials and limitations of dicotyledonous wood for climate reconstructions. *Paleobiology 19*(3): 487-498. doi: 10.1017/S009483730001410X.

United Nations. (2015). World Population Prospects The 2015 Edition: Key Findings and Advance Tables. Retrieved from https://esa.un.org/unpd/wpp/publications/files/key_findings_wpp_2015.pdf.

Zimmerman, M. H. (1983). Xylem structure and the ascent of sap. In T. Timell (Ed.), *Springer Series in Wood Science*. Berlin: Springer-Verlag.

Zhu, J., Liu, J., Lu, Z., Li, J., Sun, J. (2018). Water-use strategies of coexisting shrub species in the Yellow River Delta, China. *Canadian Journal of Forest Research 48*(9): 1099-1107. doi: 10.1139/cjfr-2018-0063.

APPENDIX

Appendix A: Modeled Sample Volume

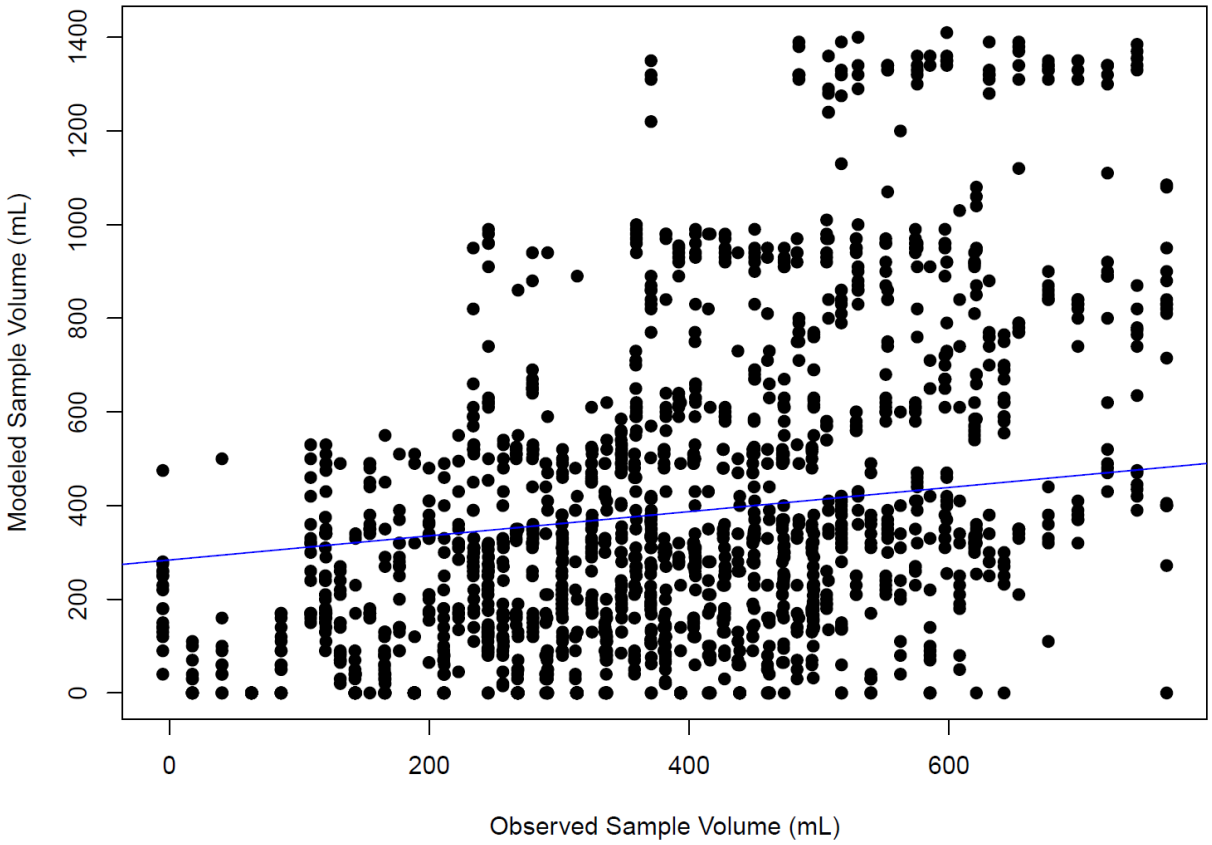

Figure A.1. Observed sample volume versus sample volume modeled by multiple linear regression (Table 2.2). The multiple linear regression line is in blue.